



University of South Bohemia in České Budějovice

Faculty of Science

Bachelor thesis

Analysis of mitochondrial bioenergetics of the  
bloodstream form of *Trypanosoma brucei*.

Laboratory of Functional Biology of Protists

Department of Molecular Biology

Mykyta Ielanskyi

2018

Supervised by RNDr. Alena Panicucci Zikova, PhD

Co-supervised by Brian Panicucci

Bachelor thesis:

Ielanskyi, M., “Analysis of mitochondrial bioenergetics of the bloodstream form of *Trypanosoma brucei*”. Bachelor of Science Thesis, Faculty of Science, University of South Bohemia, Ceske Budejovice, Czech Republic.

Annotation:

*Trypanosoma brucei* is a pleomorphic extracellular parasite that represents significant scientific interest due to its early divergence from the eukaryotic lineage and its range of unique adaptations. Among these adaptations are some metabolic pathways that are unconventional and are not fully understood. Among such pathways are the catabolic pathways of the parasite’s bloodstream form, in particular those responsible for ATP supply to the parasites’ reduced mitochondrion. This thesis investigates the nature of these pathways as well as interactions between them.

I hereby declare that I have worked on my bachelor’s thesis independently and used only the sources listed in the bibliography.

I hereby declare that, in accordance with Article 47b of Act No. 111/1998 in the valid wording, I agree with the publication of my bachelor thesis, in full form to be kept in the Faculty of Science archive, in electronic form in publicly accessible part of the STAG database operated by the University of South Bohemia in České Budějovice accessible through its web pages.

Further, I agree to the electronic publication of the comments of my supervisor and thesis opponents and the record of the proceedings and results of the thesis defense in accordance with aforementioned Act No. 111/1998. I also agree to the comparison of the text of my thesis with the Theses.cz thesis database operated by the National Registry of University Theses and a plagiarism detection system.

In Ceske Budejovice on 14.05.2018

.....

Mykyta Ielanskyi

Acknowledgements:

I would like to thank Brian for being a good and extremely tolerant supervisor as well as Geri and Alena for creating a theoretical basis for this project to exist. I appreciate the friendliness and random advices on western blots at 3 am from the whole community of the lab.

I would also like to thank Fred and Erika for making the metabolomics section of this thesis possible as well as all of the people from Bringaud lab for being hospitable hosts.

MOM, LOOK, I AM A SCIENTIST!



## Contents

1	Introduction .....	7
1.1	<i>Trypanosoma brucei</i> .....	7
1.2	<i>T. brucei</i> metabolism.....	8
1.3	Possible sources of ATP in BF parasites mitochondria .....	10
1.3.1	Transport from cytosol.....	10
1.3.2	Substrate phosphorylation inside the mitochondria .....	11
1.4	Goals.....	12
2	Materials and Methods.....	15
2.1	Cell cultures.....	15
2.1.1	Growing the cultures .....	15
2.1.2	Cell counting .....	16
2.2	Growth curves .....	17
2.3	SDS PAGE and Western blot analysis of mitochondrial succinate pathway enzymes	18
2.3.1	Harvesting cell cultures to produce whole cell lysates .....	18
2.3.2	SDS-PAGE.....	19
2.3.3	Electroblotting.....	20
2.3.4	Probing .....	21
2.4	Survival analysis in mice.....	22
2.4.1	Preparations.....	22
2.4.2	Animal work .....	23
2.4.3	Counting Parasitemia .....	23
2.5	TbAAC knockdown in SCoAS double knockout cell lines .....	24
2.5.1	Procedure.....	24
2.6	Mitochondrial membrane potential measurements .....	28
2.6.1	Procedure.....	28
2.7	Comparative metabolomic analysis.....	29
2.7.1	Sample Preparation .....	30

3	Results .....	30
3.1	Growth curves of TbAAC DKO and TbSCoAS DKO cell lines. ....	30
3.2	AAC RNAi knockdown in SCoAS double knockout.....	31
3.2.1	Cloning Results .....	31
3.3	Expression levels of enzymes involved in BF mt bioenergetics. ....	34
3.4	TbAAC DKO and TbSCoAS DKO $\Delta\psi_m$ measurements.....	37
3.5	Loss of TbSCoAS but not TbAAC decreases the virulence of <i>T. brucei</i> in mice .....	38
3.6	Metabolomic analysis. ....	40
3.6.1	Measurements.....	41
4	Discussion .....	44
5	References .....	47

**List of abbreviations used:**

BF– bloodstream form

PF – procyclic form.

NMR – nuclear magnetic resonance spectroscopy.

DKO – double knockout.

KD – knock-down.

Mt – mitochondrial

CATR – carboxyatractyloside

AAC –ATP/ADP carrier

SCoAS – Succinyl Coenzyme-A synthase

SUBPHOS – substrate phosphorylation

OXPHOS – oxydative phosphorylation

ACH – acetyl-CoA thioesterase

TDH – threonine dehydrogenase

# 1 Introduction

## 1.1 *Trypanosoma brucei*

It has been over a century now since *Trypanosoma brucei* was identified as the causative agent of African Trypanosomiasis (Castellani, Bruce and Nunes Nabarro 1903), which is also known as African sleeping sickness in humans or Nagana in livestock. According to the (World Health Organization 2016), about 60 million people in 2016 were at risk of contracting the parasite, although the number of new cases plummeted dramatically in recent years due to the implementation of more intensive disease control measures (Simarro, et al. 2011). Most of these efforts are focused on controlling the tsetse fly population, the insect vector required for the complete life cycle of this flagellated protist. Still, the currently available treatments are difficult to administer outside of hospitals and they typically cause severe side effects (Nagle, et al. 2014), prompting more research on this early diverging eukaryote to identify novel drug targets for future drug development. Furthermore, there have been examples of parasite resistance to existing drugs (Barret, et al. 2011), meaning that areas in sub-Saharan Africa where tsetse flies are widespread could once again become endemic for the debilitating disease.

Due to the ability to easily perform forward and reverse genetics in *T. brucei* (Matthews 2015), it has long been a model organism of the group Trypanosomatida, which includes other human pathogens that are the etiological agents of Chagas disease (*Trypanosoma cruzi*) and leishmaniasis (various *Leishmania* species). Several fascinating biological processes have previously been identified in *T. brucei*, such as a unique immune-evasion mechanism (MacGregor, et al. 2012), succinic acid fermentation (Bringaud, Ebikeme and Boshart 2010) and extensive mitochondrial RNA editing features (Read, Lukes and Hashimi 2016). In the Zikova lab, we are interested in the morphological and metabolic changes of the singular mitochondrion that occur throughout the complex stages of the *T. brucei* lifecycle. This extracellular parasite must traverse from the tsetse fly midgut to the salivary glands before it can be deposited back into the mammalian bloodstream. Such a drastic change of environments mandates that the parasite can easily adapt to both the glucose-rich mammalian blood and the glucose-poor environment of the tsetse fly (Smith, et al. 2017). While there have been significant advances concerning the metabolism of the axenic insect stage or procyclic form (PF) of the parasite (Bringaud, Riviere and Coustou 2006), much of our current knowledge about the axenic mammalian stage or bloodstream form (BF) is based on assays performed over 40 years ago (Vickerman, Polymorphism and mitochondrial activity in sleeping sickness trypanosomes. 1965). With new technological advancements that provide better research tools, it is important to revisit our understanding about the metabolism of this infectious stage of the parasite.

Both PF and BF can be grown axenically in culture without a need for passaging the parasite through a mammalian host or insect vector. However, these results in mostly

monomorphic parasites that are not able to fully differentiate from one lifecycle to the next. PF cells are grown in an amino acid-rich media named SDM79, while BF trypanosomes are cultured in a glucose-rich media called HMI-11. Both media are supplemented with 10% fetal bovine serum. Metabolomics studies have revealed that HMI-11 contains an excess of many nutrients that are not consumed by the parasite in culture (Creek, et al. 2013). Since *T. brucei* is quite content to generate cellular energy from a multitude of carbon sources, this artificial media changes the metabolism of the parasite from what would normally occur in nature. Therefore, recent attempts have been made to create a medium called CMM that more closely resembles what the parasite would encounter in the mammalian bloodstream (Creek, et al. 2013). However, the rate of BF proliferation is greater in the original HMI-11 media, so it is still the standard media used for most experiments. There are several strains of BF *T. brucei* that are used in the laboratories around the world. They were usually isolated from infected animals decades prior and are most often defined by the variant of the VSG expressed on its cell surface. The monomorphic Lister 427 cell line is a widely used BF trypanosome strain, mainly because it is *T. brucei brucei* and doesn't possess the genetic capacity to be infective to humans (Cross 2010).

The pleomorphic state of the natural parasite is best observed in the drastic changes of its structural morphology as it alternates between the two main lifecycle stages: PF of the tsetse fly mid-gut and the proliferative BF of the mammalian host. There are several important differences between the two life stages: mainly the expressed cell surface protein coat, the location of the mitochondrial (mt) DNA compared to the nucleus and the structure and activity of the mitochondrion. The cell surface proteins in both lifecycles are anchored to the plasma membrane via glycosyl phosphatidylinositol (GPI)-anchored proteins. The predominant protein expressed on the surface of the insect stage is procyclin, while the variable surface glycoprotein (VSG) constitutes about 20% of the total protein of the BF parasite, forming a dense coat approximately 15nm thick. The VSG acts as a defense mechanism against the host's immune system because the entire protein coat can quickly be internalized when it becomes bound by a VSG specific antibody. Through an unknown mechanism that is undoubtedly very energetically demanding, the parasite then replaces the entire surface coat with another of the numerous variants of the surface protein that are at its disposal (Horn 2014) .

## **1.2 *T. brucei* metabolism**

The mitochondria of most eukaryotes are the powerhouse of the cell because it is the organelle responsible for the generation of vast quantities of ATP by oxidative phosphorylation (OXPHOS). This holds true in the PF parasite, which has an elaborately branched mitochondrion that catabolizes the amino acids abundant in the insect's midgut - mainly proline, threonine and glutamine. These metabolic pathways feed into the incomplete, but operational citric acid cycle, which generates reduced NADH to supply the electron transport

chain (Van Weelden, et al. 2005). Respiratory complexes III and IV then create the mt membrane potential ( $\Delta\psi_m$ ) by pumping protons into the inner mt membrane space (IMS). Finally, the OXPHOS process is completed when  $F_0F_1$ -ATP synthase converts the potential energy of the proton gradient into mechanical energy as the enzyme rotates when the protons are allowed to flow down their electrochemical gradient. This rotation creates conformational changes in the catalytic site of the complex that generates ATP from ADP and inorganic phosphate (Zikova, et al. 2009). This ATP is then transported into the cytosol by the ADP/ATP carrier (TbAAC) to meet most of the parasite's energetic needs (Gnipová, et al. 2015). Among the excreted end-products of such catabolism are acetate, succinate and alanine (Smith, et al. 2017). It should also be noted that in nature it is fairly common for cells to switch to glycolysis for ATP production when they occupy environments rich with saccharides. PF trypanosomes are no exception to this, since in artificial conditions, such as a culture grown in a glucose-rich media, they tend to switch from OXPHOS to mostly glycolysis (Coustou, et al. 2008) (Smith, et al. 2017).

Both PF and BF parasites possess a peroxisome-like organelle called the glycosome. Most of the enzymes of the glycolytic pathway are localized to this unique organelle. While PF parasites grown in glucose depleted media depend on ATP generation from amino acid catabolism in the mitochondrion, the glycosomes in BF cells are almost 10-fold more active and produce almost all of the cellular ATP due to the abundance of glucose in the mammalian bloodstream (Gabaldon, Ginger and Michels 2016) (Smith, et al. 2017). The glycosomes lack the capacity to transport NAD(H) and other reducing agents, therefore they utilize shuttles to aerobically oxidize glycerol-3-phosphate (Gly-3P) into dihydroxyacetone via the mitochondrial glycerol-3-phosphate dehydrogenase (Gly-3-PDH). Interestingly, in anaerobic conditions the pathway does not function and the Gly-3P is converted to glycerol. This results in a 1:1 output of glycerol and pyruvate, both of which are excreted. However, under normal aerobic conditions, the overwhelming majority of glucose is processed into pyruvate that is excreted from the cell (Zikova, Verner and Nenarokova 2017). Meanwhile, only about 1% of the pyruvate undergoes succinic acid fermentation (Smith, et al. 2017).

However, the BF mitochondrion is reduced in structure and lacks a canonical cytochrome-mediated respiratory chain (Vickerman 1985). Therefore, the ATP synthase reverses its catalytic activity and hydrolyzes ATP to pump protons into the inner mitochondrial space. This establishes the mt membrane potential ( $\Delta\psi_m$ ) that is essential for the import of the hundreds of nuclear encoded mt proteins (Schnauffer, et al. 2005). While it has long been reported that the BF mitochondrion lacks many of the common metabolic enzymes found in PF cells, this simplistic view is now being challenged (Zikova 2017), most notably their energy production. Each of the two forms displays their adaptations to their corresponding environment. Whereas PF have active mitochondria and citric acid cycle which are required to survive the glucose deprived protein rich insect mid-gut, LS-BSF have no PHOSPHOX due to the high glucose concentration in the mammalian bloodstream (Zikova, Verner and

Nenarokova 2017). At the same time BF parasites express VSGs as a part of their adaptation to the host's immune system while PF parasites lack those energy expensive features (Smith, et al. 2017).

The mitochondrion of the BF parasite shrinks in both size and function compared to that of the PF. Most of the citric acid enzymes are still present, but and some of them are active, but the cycle itself does not function. The electron transport chain is lacking the complexes III and IV, leaving the maintenance of the proton gradient which is essential for mitochondrial protein import up to the reverse activity of the ATP-synthase, which hydrolyses ATP to translocate the protons across the inner membrane (Schnauffer, et al. 2005). TbAAC acts in reverse as well, exchanging the abundant glycolysis-derived ATP from the cytosol for matrix ADP.

On numerous occasions studies have observed minor excretion of acetate, succinate and alanine. Those have been attributed to the minor presence of SS-BSF cells which are known to possess many of the qualities of PF trypanosomes including certain aspects of metabolism (Zikova, Verner and Nenarokova 2017). The conventional theory states that AAC is the only way ATP can be obtained inside the mitochondrial matrix of the BF parasites. However, as the exploration of the mitochondrion of the BF parasite goes on, there have been several important discoveries made in the recent years, such as the fact that BF parasites excrete acetate production of which in mitochondria is essential for their de-novo fatty acid synthesis. In fact, in environments with similar glucose concentration, both forms excrete equivalent amounts of acetate derived from glucose (Mazet, et al. 2013). The article also underlines the fact that most if not all of the mitochondrial enzymes involved in the succinate and acetate branches of mitochondrial catabolism that are known in PF parasites are also expressed in BF. This suggests broader scope of catabolic activity within the mitochondrion than anticipated by older hypotheses.

### **1.3 Possible sources of ATP in BF parasites mitochondria**

#### **1.3.1 Transport from cytosol**

A key link between the mitochondrial and cytosolic metabolism is the ATP/ADP carrier (AAC). It serves normally to exchange one  $\text{ADP}^{3-}$  molecule from cytosol for one  $\text{ATP}^{4-}$  from the mitochondrial matrix. This establishes an energetic link between the source of ATP – ATP synthase within the mitochondria and the consumers in the cytosol (Taleva 2016). The transfer rate depends on the corresponding concentrations of ATP and ADP as well as on the potential difference ( $\Delta\psi$ ) of inner membrane created by proton gradient (Springett, et al. 2017).

TbAAC is known to form complexes with other proteins of the inner mitochondrial membrane in various organisms to increase the efficiency of the mitochondrial ATP production by channeling. The existing evidence indicates that in trypanosomes it functions as monomeric single-site binding transporter. In other words, it works in a “ping-pong” fashion by binding

one substrate at a time, translocating it and locking open to the other side until the other substrate binds, which is then transported to the initial side of the membrane where the transporter locks open until another molecule of the first substrate binds for cycle to repeat. In this way ATP and ADP are transported in 1:1 molar ratio without the need for  $Mg^{2+}$  or other ions to bind ADP (Traba, Satrustegui and del Arco 2009).

There are 24 mitochondrial transport proteins identified in *T. brucei* genome by sequence analysis and phylogenetic reconstruction. Most of them have been successfully localized in the mitochondria of the PF trypanosomes and assigned function based on homology of conserved sequences to proteins of yeast and humans (Colasante, et al. 2009).

Two proteins were considered to act as AAC transporters, TbMCP5 and TbMCP15. However, only TbMCP5 was proven to be a functional ATP/ADP carrier. Presumably TbMCP15 lacked a few important features of the sequences conserved across all ADP/ATP translocases. Most notably it had RRRMMI in place of RRRMMM in conserved ADP binding domain. (Pena Diaz, et al. 2012) The possible involvement in ATP transport by another protein, TbMCP6, has been disproven by functional studies. TbMCP5, being the only confirmed functional AAC in the genome, is referred to as TbAAC (Taleva 2016).

There is a number of known specific inhibitors to AACs. Most prominent are atractyloside along with its derivatives and bongkrek acid. Atractyloside derived inhibitors lock the transporter open in the c-state (open towards cytosol), while bongkrek acid locks it in m-state (open towards the mitochondrial matrix) (Kedrov, et al. 2010). These inhibitors have been useful in many experiments involving the transporter in the past, including the determination of the structure of the transporter itself (Ruprecht, et al. 2010).

As mentioned in the previous section, TbAAC functions “by the book” in the PF parasite, exchanging cytosolic ADP for mitochondrial ATP. It is essential in PF parasites causing severe growth defects when knocked down with RNAi (Pena Diaz, et al. 2012). At the same time, knockdowns in BF cell show no growth phenotype, which indicates that there might be other ways of getting ATP into the mitochondria in BF parasites (Taleva, unpublished results). The option with different transporters is unlikely due to the fact that ADP/ATP transporters have some sequence motifs that are highly conserved amongst the eukaryotes and sequence analysis performed by (Colasante, et al. 2009) would detect them.

### **1.3.2 Substrate phosphorylation inside the mitochondria**

There are two known mitochondrial SubPhos pathways capable of producing ATP in *T. brucei*, both of which involve a common step of hydrolysis of succinyl-CoA to succinate and CoASH which is coupled to synthesis of ATP from ADP and Pi. The resulting succinate is excreted while coenzyme A is recycled (Bochud-Alleman and Schneider 2002).

The enzyme succinyl Coenzyme-A synthetase (SCoAS) is a highly conserved part of the citric acid cycle. It has  $\alpha$  and  $\beta$  subunits that usually form an  $\alpha\beta$  dimer. The beta subunit is responsible for binding the substrate. The enzyme is present in a wide variety of taxa, ranging from bacteria to mammals. There are different isoforms that can take either GDP/GTP or ADP/ATP (Taleva 2016). SCoAS found in the Trypanosome genome shows sequence similarities to that found in *E.Coli*. In particular the  $\beta$  unit possesses a catalytic domain with a histidine residue in the binding motif, indicating the enzymes use  $Mg^{2+}$  for binding ATP. Removal of SCoAS  $\beta$  subunit and proteins upstream of it in the metabolic pathway has been previously considered to impact growth in trypanosomes (Zhang, et al. 2010).

The first of the pathways yields succinyl-CoA from oxidative decarboxylation of 2-oxoglutarate. The oxoglutarate is in turn derived from proline and glutamine, which are supposedly imported by mitochondrial transporters. The second pathway employs ASCT, which is normally characteristic of anaerobic organisms (Taleva 2016), to transform acetyl-CoA derived from pyruvate and threonine by the enzymes TDH and PDH to succinyl-CoA with further hydrolysis by SCoAS. The second pathway is one of the sources that feeds the essential acetate production (Zíkova, Verner and Nenarokova 2017).

#### **1.4 Goals**

As described in the previous section, there have been numerous questions arising regarding the true nature of the mitochondrial ATP in the trypanosomes. Gergana Taleva was previously successful at producing cell lines which were double knockouts of AAC and SCoAS (verbal communication). The goal of this project was to collect data about these cell lines that could help shed light on the interdependence between the different pathways including that of ATP import via AAC and SubPhos pathways the main ATP yielding component of which is SCoAS and possibly identify if there are other pathways at work.

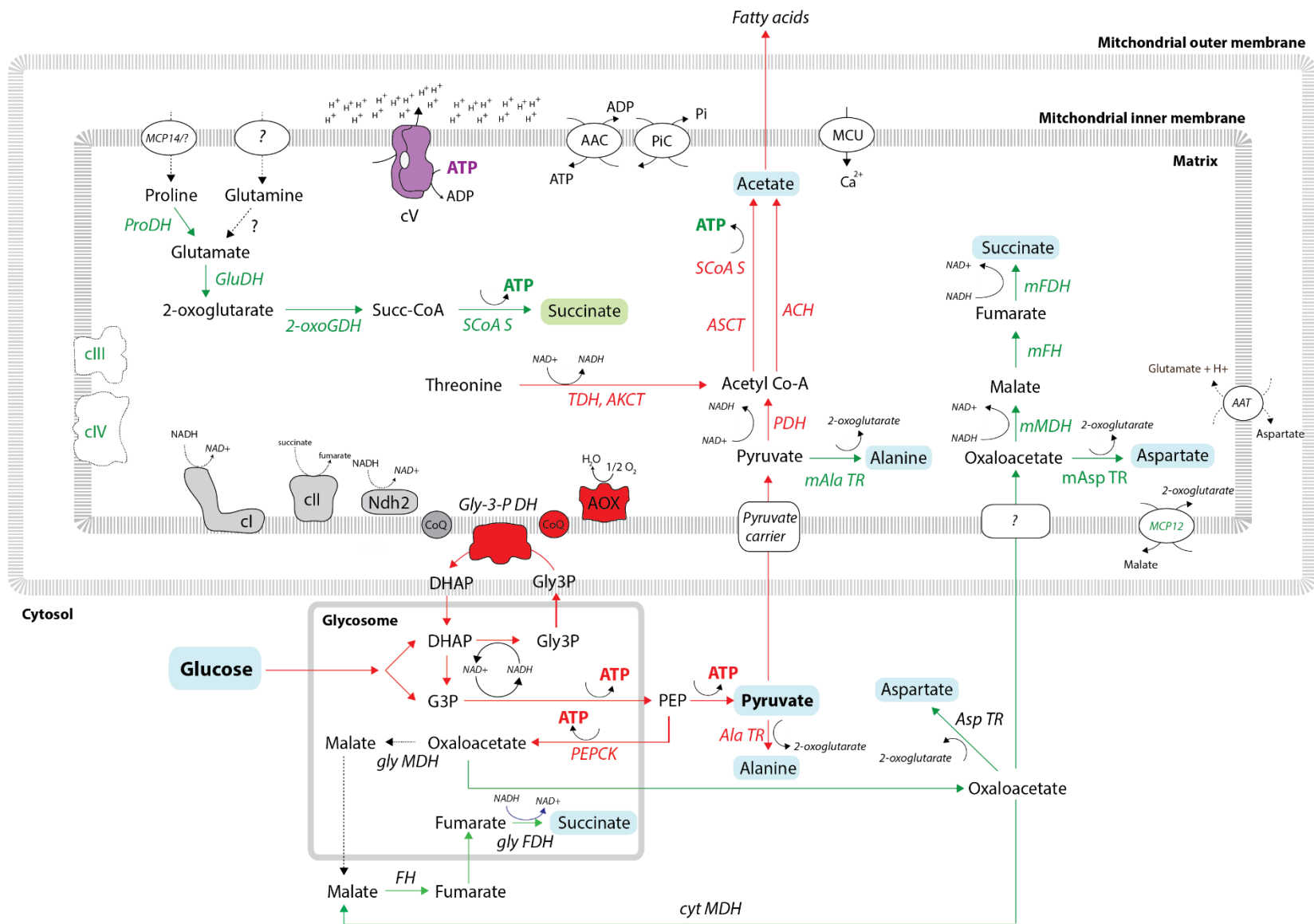


Figure 1: Proposed scheme of metabolomics of *T. brucei* mitochondrion (Zikova, Verner and Nenarokova 2017).



## 2 Materials and Methods

### 2.1 Cell cultures

Most of the experiments performed within the scope of this work required the maintenance of BF *Trypanosoma brucei* cell cultures. Therefore, it is important to specify the general conditions used to cultivate these parasites.

#### 2.1.1 Growing the cultures

BF *T. brucei* were usually grown in 5ml cultures within 25cm<sup>2</sup> plastic flasks. The flasks were kept at 37°C in an incubator constantly supplied with 5% CO<sub>2</sub> levels. Proliferating cells metabolize at high rates, releasing CO<sub>2</sub> into the media. This CO<sub>2</sub> will make the media acidic, which can be observed when the media turns a yellowish-orange color due to the presence of the pH indicator dye, phenol red. To offset this effect, sodium bicarbonate is used as a buffer in the media because dissolved CO<sub>2</sub> will be in equilibrium with bicarbonate ions. To maintain the required neutral pH of 7.3, the concentration of the sodium bicarbonate in the medium must be matched with the level of CO<sub>2</sub> in the atmosphere above the medium. Therefore, the lids to the flasks were always left vented by leaving them slightly loose.

The media was prepared from components available in the laboratory according to the following recipe:

**Table 1: HMI-11 + 10% FBS media content (Reagent recipes of Laboratory of Molecular Biology of Protists (unpublished) 2015).**

Reagent	Quantity per 10L of media
Invitrogen HMI-9 premix	181.4 g
Sodium Bicarbonate	30 g
Penicilin/Streptomycin	100 ml
The final volume adjusted with MiliQ water	9.0 L
to	
FBS	1.0 L

It is important not to stress the cultured cells, especially when they will be used to study cellular bioenergetics and metabolism. While BF parasites can easily tolerate low densities, they do not grow well at higher densities. Therefore, it is important to maintain BF *T. brucei* cultures in mid-log phase, which equates to roughly  $1 \times 10^5 - 2 \times 10^6$  cells/ml. The doubling time of axenic BF parasites is about 6-8 hours, meaning that cells could be kept perpetually in mid-log phase by splitting them 1:10 every day. However, to save costs associated with media production, BF cells were routinely split to nothing every two days if they were not needed for any experiments. The few remaining drops of cell culture left behind in the flask were sufficient to seed the culture for another two days of growth in 5ml of fresh media.

Every time the cells were to be split, the morphology and motility of the cells was observed under a Zeiss Primo Vert optical microscope using a 20X magnification. Healthy BF parasites should be moving rapidly in a tumbling manner. There should also be several parasites dividing in one field of view. This phenomenon can be observed as two flagellated parasites that are still adjoined at their very posterior ends. Signs of stress should also be monitored. Unfavorable conditions can manifest in rounded cells, long thin cells or groups of cells in a rosetta-like aggregation. Finally, great precautions should be taken upon every manipulation of the cell cultures to ensure that they do not get contaminated with any bacteria or fungi. The best way to eliminate this possibility is to perform aseptic techniques within the tissue culture hood.

### 2.1.2 Cell counting

Since the density of a cell cultures was one of the crucial parameters in virtually every experiment within the scope of this work, keeping an accurate track of this parameter was of utmost importance. In order to obtain accurate cell density values for the BF trypanosome cultures, a Z2 Coulter Cell counter was used.

Coulter cell counters force cells to form a single file line in a microchannel by passing them through a narrow aperture. A voltage is then applied through the microchannel and the detector counts a cell whenever the voltage drops due to the passage of a cell (Coulter 1949). After counting cells in a known volume, we can calculate the cells density of the cell culture. The size of the cell can be entered into the computer so it knows if the duration of a voltage drop was due to a particle of interest. Since BF *T. brucei* resemble corkscrews, they can enter the microchannel in a wide variety of orientations, anything from a vertical line to a horizontal line. Therefore, we have set up a wide gating system from 3.5-7.5uM to produce cell counts obtained by eye on a hemocytometer.

Samples were prepared for measurements by thoroughly mixing 100ul of the culture with 100ul of Trypanosomatid Cell Fix solution (Table 2) in a 1.5ml test tube. The formaldehyde fixed the proteins of the cell, rendering them intact but not infectious to any future users of the counter. 50ul of the fixed cells were then added to a cuvette containing 5ml of isotonic Hemosol. The cuvette was loaded onto the platform, which was raised to submerge the aperture into the cell solution. The counting was initiated and a final concentration in cells/ml was calculated by the computer based on the dilution factor entered into the program.

**Table 2: Preparation of Trypanosomatid Cell Fix solution (TrypFix).**

<b>Reagent</b>	<b>Stock</b>	<b>Amount</b>	<b>Final</b>
<b>Distilled H<sub>2</sub>O</b>		85ml	-
<b>SSC</b>	20x	5ml	1x
<b>Formaldehyde</b>	36%	10ml	3.6%

## 2.2 Growth curves

To determine if the elimination of a gene product has any effect on the proliferation rate of the resulting cell line, we measured the cumulative density of the cell population over a period of seven days. The liquid nitrogen stabilates of each clonal cell line were thawed and allowed to acclimate to growth in a new TC flask. Care was taken to start the growth curves shortly after the first week of growth, which limited the potential effects that long-term culturing might have on the malleable metabolism of the parasite. The cell populations were counted on Z2 Coulter counter and split on a daily basis, preferably every 24 hours. The cells were kept in mid-log phase by splitting the 5ml population to  $2 \times 10^5$  cells/ml. The following calculations were made in an Excel sheet to determine how much of the cell culture should remain in the flask and how much fresh media should be applied.

$$V_{left} = \frac{n_{needed}}{C_{counted}}$$

**Equation 1: Calculating volume of the culture to be left.**

$$V_{dilute} = 5ml - V_{left}$$

**Equation 2: Calculating the volume of media to be added (Vdilute).**

The densities recorded in the Excel sheet were then used to calculate the cumulative density of the culture as if they were growing in a theoretical flask that was sufficiently large enough to eliminate the need to remove any of the culture over the period of the growth curve. The following calculations were thus incorporated into the Excel sheet.

$$f_{dilution} = \frac{5ml}{V_{left}}$$

**Equation 3: Calculating dilution.**

$$f_{cumulative} = f_{cumulative\ yesterday} * f_{dilution}$$

**Equation 4: Calculating cumulative dilution using previous value and current dilution.**

$$C_{cumulative} = C_{counted} * f_{cumulative}$$

**Equation 5: Calculating current concentration.**

The initial values for the dilution and cumulative density of the cultures on day 0 were taken as 1 and  $2 \times 10^5$ , respectively. If there is no growth phenotype, the resulting growth curves should appear linear on the logarithmic scale given the exponential nature of cell growth.

## **2.3 SDS PAGE and Western blot analysis of mitochondrial succinate pathway enzymes**

### **2.3.1 Harvesting cell cultures to produce whole cell lysates**

In order to determine if the genetically modified cells lines used in this study possessed altered expression levels of proteins involved in particular bioenergetics processes or metabolic pathways, we performed western blot analyses using antibodies generated in the lab to specific protein targets. First we need to generate whole cell lysates (WCL), which are simply harvested cell pellets resuspended in an sodium dodecyl sulfate (SDS) polyacrylamide gel electrophoresis (PAGE) buffer (SDS 2%; DTT 100mM, Tris 50mM, Glycerol 10%; Bromophenol Blue 0.006%). SDS is an anionic surfactant that disrupts the cellular membranes and coats proteins. Because of its negative charge, it denatures proteins and provides a consistent charge that allows them to migrate during PAGE according to their apparent molecular weight. To ensure that we can detect the specific antigen of interest, a WCL sample that represents between  $3 \times 10^6$  and  $1 \times 10^7$  cell equivalents is loaded in a well. Therefore, we need to harvest a large enough culture of BF parasites for multiple samples, but the populations must also be in mid-log phase in order to avoid possible metabolic anomalies that occur when high densities of cells deplete the pool of nutrients available in the media.

Therefore, we scaled up the cell lines to be investigated two days before harvesting by seeding a  $150\text{cm}^2$  flask with  $5 \times 10^6$  total cells in a final volume of 30ml fresh media. The next day we further expanded the cultures by seeding a 150ml of total media with a total of  $5 \times 10^6$  cells. On the third day, the cells were counted twice and the values were averaged to yield a more accurate count. This helped to ensure that we were preparing WCL of equal cell equivalents for each cell line, which would aid the normalization process performed later. Calculated volumes corresponding to equal numbers of cells were transferred to 250ml centrifuge conicals and balanced with media. The cells were then spun down at  $1300 \times g$  for 10 minutes at  $4^\circ\text{C}$ . The media was discarded immediately after the run and the containers were placed on ice. The cell pellets were resuspended in 50 ml chilled phosphate buffered saline (PBS) containing 0.01% glucose (PBS-G). The cell suspension was then transferred to 50 ml conicals and then centrifuged again at  $1300 \times g$  for 10 mins at  $4^\circ\text{C}$  to remove any traces of protein from the media. The supernatant was once again discarded; the cell pellet resuspended in 1ml PBS-G was transferred to a 1.5 ml Eppendorf tube and centrifuged one more time at  $1300 \times g$  for 10 minutes at  $4^\circ\text{C}$ . The final cell pellet was resuspended in 1x PBS before a 3x SDS loading dye buffer was added. These volumes were calculated so that 30ul of this final WCL would be the equivalent of  $1 \times 10^7$  cells. The lysate was then heated at  $97^\circ\text{C}$  for 7-9 minutes and mixed carefully to ensure the proteins were denatured and the genomic DNA sheared. The resulting lysates were then stored in the  $-20^\circ\text{C}$  freezer until they were required for western blot analysis.

### 2.3.2 SDS-PAGE

SDS-PAGE provides a way to separate all the proteins of a cell according to their molecular weight. When the negatively charged, denatured protein samples are placed in an electric field, they traverse to the anode by migrating through a labyrinth of small molecular holes created by crosslinking acrylamide polymers. Therefore, larger proteins will migrate more slowly than smaller proteins. For these experiments, we chose to use the Mini-PROTEAN TGX Stain-Free AnyKD™ Tris-Glycine gels from BioRad. These uniform gels contain a gradient of acrylamide that allow for good resolution of any proteins between 10-100 kDa. They also have an extra advantage in that the TGX chemistry allows the user to visualize the resolved proteins in the gel using a UV light, which is useful to normalize data obtained from various cell lines. The gels were placed in a Bio-Rad Mini-PROTEAN Tetra Cell electrophoresis unit according to the manufacturer's instructions. Each well was loaded with 20ul of WCLs (equivalent to  $\sim 6 \times 10^6$  cell). 4ul of the PageRuler™ pre-stained protein ladder (Figure 2) was also loaded to determine the molecular weight of any detected proteins in the western blot analysis. The whole electrophoresis unit was then placed in a 4°C refrigerator and set to apply a constant voltage of 100V. The electric field was applied until the dye front of bromophenol blue in the SDS PAGE loading buffer exited the bottom of the gel. The gels were then removed from the casing and photographed on the Bio-Rad Chemidoc using the Stain-Free presetting (Bio-Rad Laboratories 2012) to record the protein profile of each sample, which can be used later for normalization.

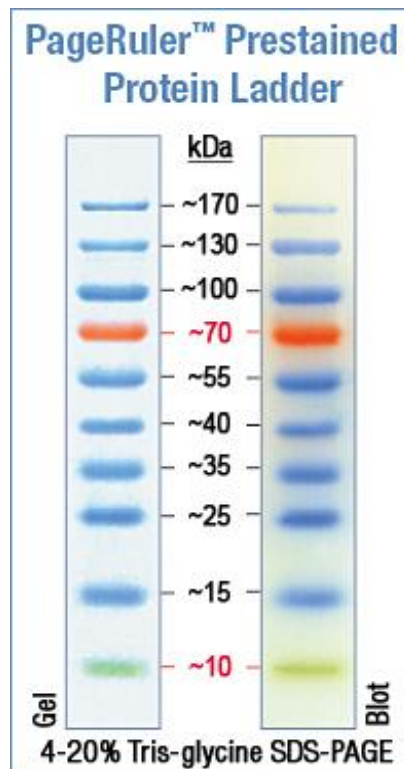


Figure 2: PageRuler™ pre-stained protein ladder.

### 2.3.3 Electroblothing

Protein immunoblotting is a technique commonly used in molecular biology to transfer proteins onto a polyvinylidene difluoride (PVDF) or nitrocellulose membrane, which provides a more rugged platform to probe the resolved proteins with specific antibodies. These membranes can be probed with several different antibodies if the targets differ in size and the respective antibodies produce clean signals of similar intensity. Otherwise it is best to sequentially probe the blot over a span of several days. However, the signal detection will decrease over time as the retention of the absorbed proteins becomes weaker. It is also important not to touch the membrane with your bare hands as this will deposit fatty acids that will interfere with the detection of your target protein.

To facilitate the efficient transfer of the proteins from the polyacrylamide gel onto a PVDF membrane, a solid support sandwich is created around the membrane and gel (Figure 3). All the necessary layers of the sandwich are first equilibrated in 1x transfer buffer (Glycine 9.76g/l, Tris base 19.4g/l) before the assembly of the transfer stack. In addition, due to the high hydrophobicity of the PVDF membrane, it must first be charged in methanol for 40 seconds, then washed in MilliQ water for 2 minutes and finally equilibrated in the transfer buffer. The assembled transfer stack is then placed in a transfer tank and immersed in transfer buffer. Efficient transfer of most proteins can be achieved by applying 90V for 90 minutes. To minimize the damage created by the heat generated during this process, the transfer tank should be kept cold with either an ice pad or by placing the apparatus in a 4°C refrigerator. Once the transfer was completed, the stack was removed from the bath and carefully disassembled. Gels and membranes were visually inspected to determine if there had been an efficient transfer of the various prestained proteins that comprise the molecular weight ladder.

## Transfer Stack

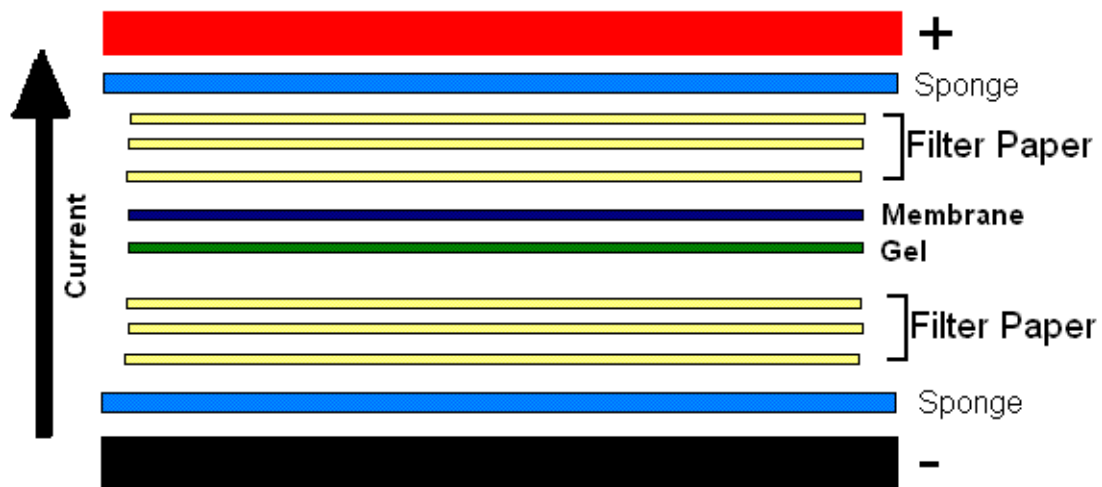


Figure 3: General idea of electroblotting "sandwich"(public domain image according to (Dubey 2014)).

### 2.3.4 Probing

While the membranes provide a solid support system for the proteins, they must not be allowed to get dried out. As soon as the membranes are disassembled from the transfer stack, they are placed in a 50 ml conical and blocked overnight with 5% skim milk dissolved in a PBS solution with 0.05% tween (PBS-T). The following day, specific primary antibodies are diluted into fresh 5% milk PBS-T. Table 2 indicates the dilutions used for each antibody. These values were determined based on previous experience using similar amounts of WCL. The membranes were incubated at room temperature for 1 hour and then incubated in a series of PBS-T washes (2x quick wash in 25 ml PBS-T, one 15 min wash in 25 ml and 2x 5 min washes with 25 ml). These washes are needed to remove the antibodies that did not bind the proteins on the membrane and to prevent them from binding non-specifically over time.

Table 3: Order and dilutions of antibody probes for each type of WB performed.

Cell line	Target protein	Antibodies (primary, secondary)
AAC DKO	ASCT / day 1	Rabbit ASCT(1:1000), Goat anti-rabbit HRP (1:2000)
	ASCT / day 2	Rabbit P18(1:500), Goat anti-rabbit HRP (1:2000)
	ASCT / day 3	Mouse mtHSP70(1:1000), Goat anti-mouse HRP (1:2000)
AAC DKO	TDH / day 1	Rabbit TDH(1:500), Goat anti-rabbit HRP (1:2000)
	TDH / day 2	Rabbit P18(1:500), Goat anti-rabbit HRP (1:2000)

	TDH / day 3	Mouse anti-mtHSP70(1:1000), Goat anti-mouse HRP (1:2000)
<b>SCoAS DKO</b>	AAC / day 1	Rabbit AAC(1:1000), Goat anti-rabbit HRP (1:2000)
	AAC / day 2	Rabbit P18(1:1000), Goat anti-rabbit HRP (1:2000)
	AAC / day 3	Rabbit ASCT(1:1000), Goat anti-rabbit HRP (1:2000)
	AAC / day 4	Mouse mtHSP70(1:1000), Goat anti-mouse HRP (1:2000)

**Table 4: Sizes of the investigated proteins.**

<b>Protein</b>	<b>Size (kDa)</b>
<b>mtHSP70</b>	70
<b>ASCT</b>	53
<b>TDH</b>	36.5
<b>AAC</b>	34
<b>P18</b>	18

To detect the binding of the primary antibody to the target protein, the membrane is next incubated for 1 hour with a secondary antibody. The primary antibodies are typically either from rabbits (polyclonal) or mice (monoclonal), so the secondary antibody is usually generated in a goat and it recognizes any rabbit or mouse primary antibody. After incubation with the secondary antibody, the membranes are again washed with PBS-T as described above. The secondary antibody is labeled with horseradish peroxidase (HRP), which creates a chemiluminescent signal when the Bio-Rad Clarity western ECL substrate covers the membrane. This ECL kit is comprised of two reagents that need to be mixed in a 1:1 ratio. Then 500 ul of the ECL reagent are applied to each membrane and allowed to incubate for 1 minute. Excess ECL substrate is carefully removed and the blots are visualized on the Bio-Rad Chemidoc imager. The resulting digital images were then quantified using ImageLab software. This quantification data was further processed using Microsoft Excel to calculate the statistics.

## **2.4 Survival analysis in mice**

### **2.4.1 Preparations**

Since the energetic demands of the parasite in an axenic culture are presumably lower than in an animal model with an active immune system, Balb/c mice were infected with various BF *T. brucei* cell lines and monitored for the parasitemia levels. Relevant cell lines were thawed from liquid nitrogen stabilates and cultivated in culture for a brief time to ensure that the parasites were consistently growing at mid log phase for several days. To prepare cell lines

for infecting the mice,  $1 \times 10^6$  cells were harvested by spinning at 1300xg for 10 minutes at room temperature. This cell pellet was then resuspended in 1ml of PBS-G.

#### 2.4.2 Animal work

All the animal work in this section was performed by a properly authorized and qualified professional. All of the animals involved have been treated and disposed of according to the standards of acting legislation of the Czech Republic and the European Union. Great care was taken to make sure that the animals experienced minimal stress and they were sedated when blood samples were obtained. Finally, the animals were sacrificed with an overdose of ether once they looked moribund or the parasitemia levels surpassed  $1 \times 10^8$  parasites/ml.

The mice used in the experiment were female BALB/c mice that were at least 6 weeks old. Littermates were split into cages consisting of 5-7 mice. On day 0, the mice were infected with  $1 \times 10^5$  parasites (~ 0.1 ml) intraperitoneally. Blood samples obtained from tail pricks were collected daily. The mice were first sedated with 20ul/g body weight of the approved sedative listed in Table 5. Then 2ul of blood was instantly mixed with 198ul of TrypFix solution in order to preserve the sample until they could be counted.

**Table 5: Recipe for the sedative for mice.**

<b>Reagent</b>	<b>[Stock]</b>	<b>2 ml</b>
<b>NaCl</b>	0.9%	1.4 ml
<b>Narketan</b>	100 mg/ml	400 ul
<b>Rometar</b>	20 mg/ml	200 ul

#### 2.4.3 Counting Parasitemia

The blood samples were counted on a 0.1 ul Counting Chamber CE Neubauer-IMP DL. The number of cells counted in all 25 center squares was multiplied by  $10^6$  in order to obtain the per milliliter concentration of parasites in the blood. Microsoft Excel and GraphPad Prism were used to calculate the statistics and graph the results. Microsoft Excel and GraphPad Prism were used to calculate the statistics and graph the results.

## 2.5 TbAAC knockdown in SCoAS double knockout cell lines

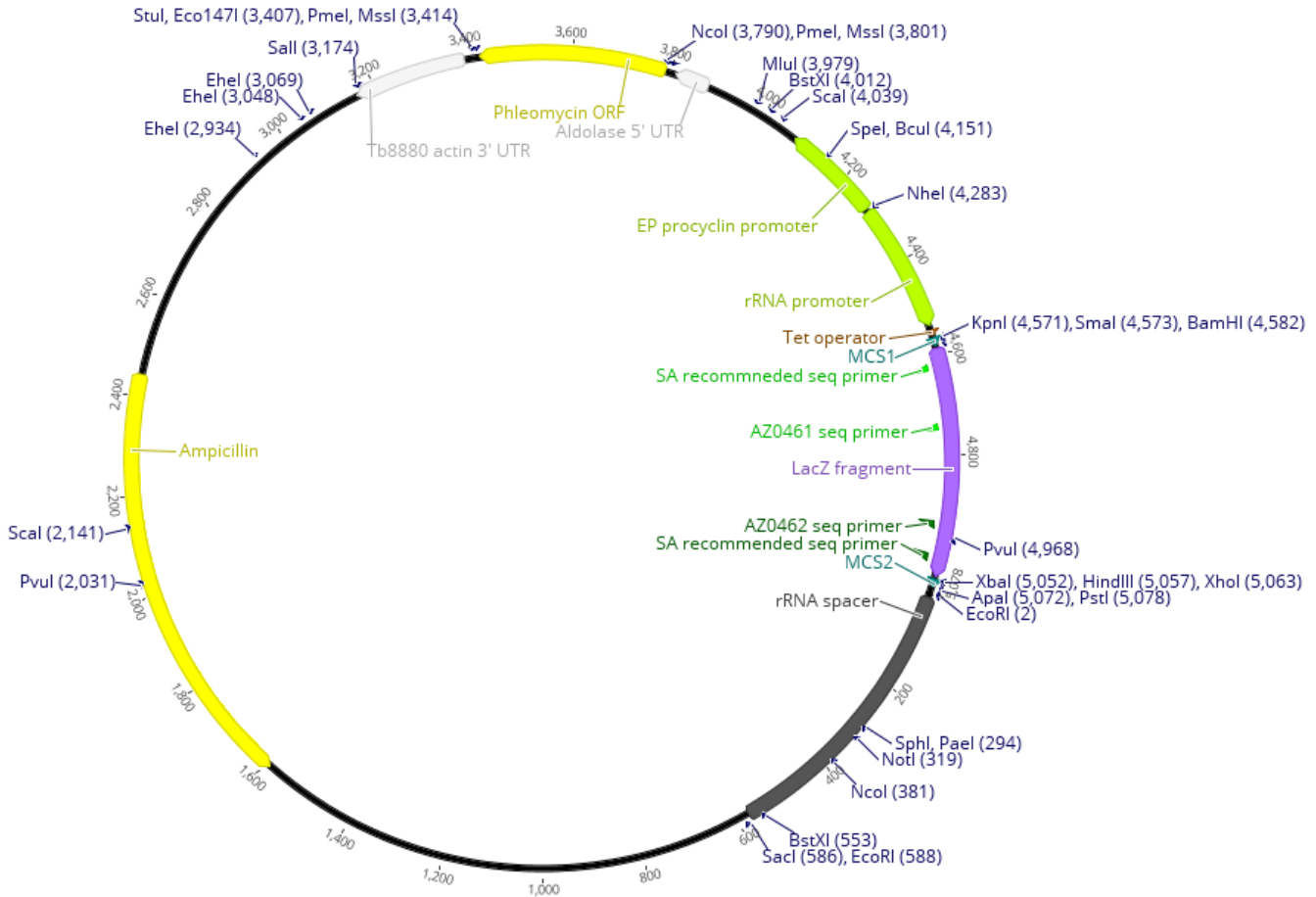


Figure 4: pAZ55 plasmid map.

### 2.5.1 Procedure

#### 2.5.1.1 Cloning pAZ055 TbAAC RNAi

Preliminary data suggests that the functions of TbAAC and TbSCoAS may overlap in cultivated BF *T. brucei*. To verify this possibility, we wanted to deplete TbAAC in the TbSCoAS DKO cell line. To generate a robust knockdown, we cloned TbAAC into the stem loop RNAi vector named pAZ055. This requires the insert of the TbAAC RNAi PCR fragment into the first multiple cloning site (MCS1) and then performing a second ligation to insert the same PCR fragment in the reverse orientation at MCS2. A previous lab member had already generated the pAZ055 plasmid containing the TbAAC RNAi fragment at MCS1.

To continue with this cloning process, we transformed the pAZ055 MCS1 TbAAC RNAi plasmid into competent XL-1 Blue chemically competent cells. This process involved

gently thawing the competent cells on ice for 15 minutes before incubating them for 10 minutes on ice with 0.5ul of the pAZ055 MCS1 TbAAC RNAi plasmid. The cells were incubated at 42°C for 45 seconds. Following this heat shock, they were allowed to recover on ice for 2 minutes. 250ul of rich SOC media was then added to the transformed cells and they were placed in a shaking incubator at 37°C. After that initial growth stage, 100 ul of transformed cells were spread on an agar plate containing 100mg/ml ampicillin, which was then placed in a 37°C incubator overnight. The next day, a single colony was selected from the plate and used to inoculate 50ml of Luria broth (LB: Bacto-Tryptone 10g/l; Bacto-Yeast extract 5g/l; NaCl 5g/l; pH ~ 7.25) containing 100mg/ml ampicillin. After shaking in a 37°C incubator overnight, a Sigma GenElute Midiprep kit was used to isolate the pAZ055 MSC1 TbAAC RNAi plasmid according to the user guide provided by the manufacturer (Sigma Aldrich Co. 2009). The purified plasmid was then quantified using a Nanodrop 3300 unit.

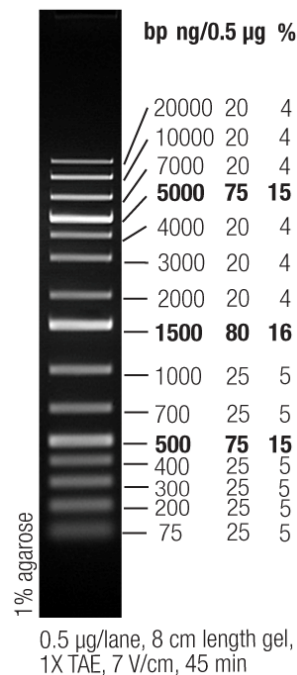


**Figure 5: 1Kb Plus prestained DNA ladder used for all of the agarose gels in the experiments (Thermo Fischer Scientific 2012).**

A PCR reaction using the primers AZ0804 & AZ0805 (Figure 6) was used to amplify the TbAAC RNAi fragment from genomic DNA previously isolated from BF WT427 Trypanosomes. The primers consist of 16-18 nucleotides (nt) that are complementary to a region of the TbAAC coding sequence. The primers also have restriction sites incorporated at the 5' ends. These were designed to match the restriction sites available in both MCS1 & 2 for sequential and directional cloning. The 50ul PCR reaction consisted of 1ul of the Taq-purpl

DNA polymerase, 5ul of the supplied 10x “Blue Buffer”, 200uM dNTP’s, 0.2 uM of each primer and 200ng of genomic DNA. The incubation temperatures and times for the denaturing and elongation steps were set according to the manufacturer’s recommendations for the DNA polymerase. The annealing temperature for the primers was set to 45°C for the first three cycles and 55°C for the last 27. The resulting pcr product was resolved at 90V for 1 hour on a 1% agarose gel . A Sigma GenElute Gel Extraction Kit was used to extract the PCR product from the agarose gel by following the manufacturer’s recommendations.

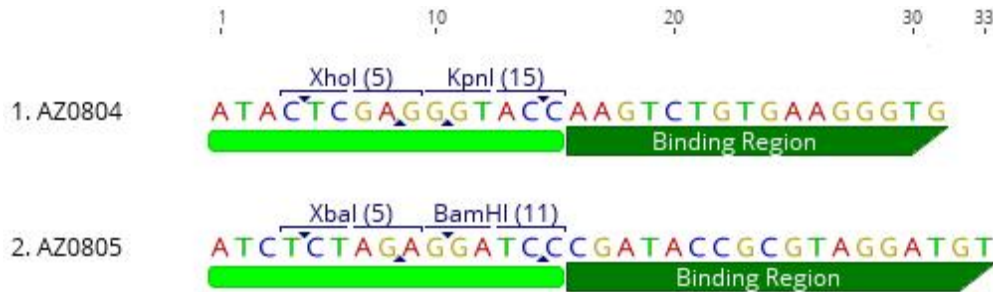


**Figure 6: Forward (AZ0804) and reverse (AZ0805) primers used to amplify a TbAAC RNAi fragment that could be easily cloned into pAZ055.**

Next, we need to create compatible 5’and 3’ DNA overhangs on both the pAZ055 MCS1 TbAAC RNAi plasmid and the TbAAC RNAi amplicon. To achieve this, both were digested with XhoI & XbaI. The digested plasmid was resolved on an agarose gel (0.8%, 0.5x TAE, 90V) and the DNA fragment of expected size was extracted from the gel using the GenElute gel extraction kit. Meanwhile, the digested PCR product was purified with the Sigma GenElute PCR Clean-Up kit according to the corresponding user’s manual (Sigma Aldrich Co. n.d.). The concentration of the linearized vector and the digested PCR fragment was then measured on the NanoDrop. These values were then used to calculate the molarity of each DNA molecule, so that the 10ul ligation reaction would consist of a 3:1 insert to vector molarity ratio. The DNA was then ligated with 1ul T4 DNA ligase and 1ul of the corresponding 10x buffer. The reaction was allowed to proceed overnight at 4°C.

### 2.5.1.2 Transfection

The ligated product was then transformed into XL-1 Blue chemically competent cells that were spread on an LB ampicillin plate. To verify if the resulting transformants contained the correct plasmid, several colonies were picked the next day and grown overnight at 37°C in LB-media with ampicillin. After isolating the plasmids with the GenElute HP Plasmid Miniprep Kit, they were subjected to a restriction digest analysis using either the enzyme pair KpnI and BamHI or XhoI and XbaI. The digested DNA was then analyzed on an agarose gel and plasmids from specific bacterial colonies were sequenced with primers AZ0461 and AZ0462 that anneal to the β-galactosidase stuffer fragment. BF T. brucei Transfections

Now that we have generated the pAZ055 TbAAC RNAi plasmid, we would like to transfect it into the BF *T. brucei* TbSCoAS DKO cell line, where it will undergo homologous recombination and integrate into the ribosomal RNA spacer locus. First, we used the Sigma GenElute Plasmid Midiprep Kit to isolate large quantities of the pAZ055 plasmid from a 50 ml bacterial culture grown overnight in a shaking 37°C incubator. The plasmid was then linearized with the NotI enzyme (50ul reaction volume, 5ul enzyme, 5ul 10x buffer and 20ug of plasmid). The resulting linear plasmid was precipitated with 1/10<sup>th</sup> volume 3M Sodium Acetate, pH 5.2 and 2.5x volumes of chilled 97% ethanol. After 30 minute incubation at -80°C, the DNA was pelleted at 4°C with a 30 minute spin at maximum speed in an Eppendorf 5424R tabletop centrifuge. The DNA pellet was then washed in 70% ethanol before it was resuspended in 30ul of sterile MilliQ water in the sterile confines of a tissue culture hood. The concentration of the linearized plasmid was measured on the Nanodrop and 1ul was analyzed on an agarose gel to verify that the digestion was complete.

Next, we prepared the BF TbSCoAS DKO clone B1 for transfection. The cells were expanded to a larger 75cm<sup>2</sup> flask and allowed to condition the flask for a day before they were expanded to a 60ml culture. The day prior to the transfection, the cells were split in a manner so they would remain in mid-log growth phase (6-8 x10<sup>5</sup> cells/ml) by the following afternoon. At which point 3x10<sup>7</sup> cells were harvested by centrifugation at 1300xg for 10 minutes at room temperature. The cell pellet was then washed with 20 ml of sterile PBS-G and resuspended in 100ul of the AMAXA Human T-Cell solution prepared from 81.2ul of the Human T-Cell Nucleofactor solution and 18.2ul of the Supplement. While the cells were being prepared, 10-12 ug of the linearized DNA was loaded into a sterile 2mm gap electro cuvette. Then 100ul of the resuspended cells were added to the cuvette, which was loaded into the AMAXA Nucleofactor II Electroporator. Using the manufacturer's preset X-001 program, the trypanosomes were electroporated. The transfected cells were removed from the cuvette and placed in 30ml of HMI-11 media containing the appropriate selectable antibiotic markers required by the parental cell line. In an attempt to select for positively transfected cell populations that arise from a small pool of original cells, we make these cells more clonal by performing two 1:10 serial dilutions. Each of these three diluted cultures were then plated out in separate sterile 24 well plates, with each well containing 1ml of cells.

After 16 hours of incubation at 37°C, an additional 1ml of media was added to the wells on each plate. However, this media contained the normal concentration of the antibiotics required by the parental cell line plus a 2x concentrated antibiotic that selects for the newly integrated ectopic DNA. A plate of the parental cells transfected without any of the linearized DNA was also created. After 4-6 days when these cells were dead due to the addition of the selectable antibiotic, individual wells from the plates with *T. brucei* transfected with DNA were monitored closely for positive selection. Cell populations with good morphology and density were eventually split in sequentially more aggressive dilutions. When they were able to repopulate a well in one day after being split 1:10, they were expanded into a 5ml culture in a

25cm<sup>2</sup> flask. After these new flasks were split several times and growing at consistent rates, long-term storage stabilates were created. Each cell population was mixed 1:1 with a trypanosome freezing solution (Glucose 19g/l; NaCl 4.2g/l; Trisodium Citrate 1.5g/l; BSA (Bovine Serum Albumin) 1g/l; Glycerol 150g/l) in a cryovial, cooled on ice for 30 minutes and then placed in the -80°C freezer for 3 days. Then the stabilates were transferred to a liquid nitrogen tank. All of these operations were performed under sterile conditions.

## 2.6 Mitochondrial membrane potential measurements

When analyzing the metabolic and bioenergetic properties of the BF *T. brucei* mitochondrion, an informative phenotypic assay involves measuring the mt membrane potential ( $\Delta\psi_m$ ). This process is essential for the organellar import of nuclear encoded mt proteins. Due to the unique bioenergetics of the BF mitochondrion, the proton gradient across the mt inner membrane is principally created by F<sub>0</sub>F<sub>1</sub>-ATPase and the biochemical pathway that supplies this enzyme with its substrate ATP.

Tetramethylrhodamine ethyl ester (TMRE) is one of the best compounds for in-situ measurements of mitochondrial membrane potential. (Thermo Fischer Scientific n.d.) TMRE is a cell permeable, positively charged fluorescent dye that accumulates in the mitochondria. The intensity of the fluorescence is relative to the  $\Delta\psi_m$ , as a larger proton gradient across the inner mt membrane space will create a more negative charge in the matrix that attracts more TMRE. To verify that the TMRE fluorescence measured in the cells is actually due to the active pumping of protons into the IMS, carbonyl cyanide-4-(trifluoromethoxy)phenylhydrazone (FCCP) is added to the cells as a negative control. FCCP is a proton ionophore (National Center for Biotechnology Information 2005) that can facilitate the transport of positively charged hydrogen ions across a lipid bilayer, causing the mt inner membrane to become depolarized. The resulting fluorescence of these cells is then measured by Fluorescence Activated Cell Sorting (FACS), which is a flexible method of analyzing fluorescent cells en-masse.

### 2.6.1 Procedure

#### 2.6.1.1 Cell cultures

The relevant cell cultures were strictly maintained at mid-log densities for 3-4 days prior to the experiments to ensure that the cultures consisted of healthy parasites with good morphology and motility. With good motilities It is important to prevent the cultures from becoming too dense, at which point specific metabolites in the media may become limiting and alter the metabolism of the parasites.. Every cell line was grown in triplicate flasks in order to statistically show that the data is reproducible.

### 2.6.1.2 TMRE staining

Each 10ml culture had densities of  $0.7-1 \times 10^6$  cells/ml.  $3-4 \times 10^6$  total cells were harvested by centrifugation at 1300 xg for 10 minutes at room temperature. The cell pellet was thoroughly resuspended in HMI-11 media containing 60nM TMRE (10ul of the stock 60uM TMRE solution in DMSO / 10ml of HMI-11). For the negative control, an equivalent number of harvested cells from the same flask were resuspended in HMI-11 containing 60nM TMRE and 20uM FCCP (20ul of 10mM FCCP stock / 10ml HMI-11). The resuspended cells were then incubated for 30 minutes in a 37°C incubator with 5% CO<sub>2</sub>. The cells were pelleted again and resuspended in PBS (1ml /  $10^6$  cells harvested). 1ml of this cell suspension was then distributed into a FACS tube.

### 2.6.1.3 FACS operation

A FACSCanto II flow cytometer was used. The cytometer possesses two lasers: blue at 488nm and red at 633nm. Proper setup of the machine was executed per manufacturer's recommendations. The settings used were the ones previously established for measuring TMRE stained BF *T. brucei* cells: the parameters were set as per Table 6 with FSC threshold of 5000. The measurements were performed as quickly as possible in order to prevent the negative effects of fluorescence decay due to cell death. A tight grouping of cells positioned along a diagonal of a forward scatter versus side scatter plot represented a population of cells with a homogeneous morphology. The resulting data was exported into a Microsoft Excel spreadsheet for further analysis.

**Table 6: Parameters of FACSCanto II flow cytometer used for the measurements of the mitochondrial membrane potential.**

Parameter	Type	Voltage
FSC	A, H, W	220
SSC	A, H, W	430
FITC	A, H, W	601
PE	A, H, W	663
PE-Texas Red	A, H, W	659
PerCP-C	A, H, W	587
PE-Cy7	A, H, W	770
APC	A, H, W	552
Alexa700	A, H, W	730
APC-Cy7	A, H, W	620

## 2.7 Comparative metabolomic analysis

NMR is an effective and flexible instrument of metabolomics. The difference in spin of nuclei with different mass enables differentiation of the products of metabolism of carbon sources labeled with introduction of one or several C<sup>13</sup> atoms in specific locations of the

substrate molecules. This allows NMR to be used not only to obtain the general picture of the products excreted during cellular metabolism, but also to trace back the pathways that yielded the metabolites. Along with the ERETIC technology which allows to substitute internal reference signal with an artificial signal to deal adequately with matrix interference of the samples, NMR metabolomics enable the use of a range of interesting techniques in combination with reverse genetics to be used to determine metabolomics pathways of the organisms (Bringaud, et al. 2015).

### **2.7.1 Sample Preparation**

The cell cultures for this particular experiment were grown in 150cm<sup>2</sup> flasks in volumes of approximately 100ml-200ml to a final density of 1-2 x10<sup>6</sup>. Aliquots of each culture were used to determine the cell density while the cells were centrifuged at 2000 rpm for 15 minutes at room temperature. The cells were resuspended in 4 ml PBS for every 10<sup>8</sup> cells harvested. 1mM of the corresponding carbon source (whether labeled or unlabeled) was added to provide a energy source for the cells, which were centrifuged again. The cell pellet was resuspended in 2-4 ml of PBS containing ~4mM of each carbon source. This volume of PBS was determined so that the resulting cell density was at least 1x10<sup>7</sup>/ml and there was enough material to conduct the experiments. This cell suspension was again quickly counted and the total volume was adjusted with the appropriate solutions so that each sample contained 10<sup>7</sup> cells/ml. These cells were aliquoted onto 24 well plates, with each well containing 1ml of cells. The plates were incubated at 37°C and 5% CO<sub>2</sub> for 2-3 hours or until the cells started to clump (the plates were monitored approximately every half of an hour). Longer incubation times in theory could provide better distinguishable metabolite bands, but the metabolites released from dying or dead cells would pollute the spectrum. Those two factors mandated an individual approach to the incubation duration during every experiment. Once the incubation is complete, the content of the wells is quickly transferred to the Eppendorf tubes and centrifuged in a tabletop centrifuge at 8000xg for 1 minute at room temperature. The supernatant is collected and stored in a -20°C freezer. About 200ul of this sample is required for one NMR measurement.

## **3 Results**

### **3.1 Growth curves of TbAAC DKO and TbSCoAS DKO cell lines.**

The TbAAC and TbSCoAS DKO cell lines were successfully generated previously in the lab, demonstrating that neither gene product was essential for *T. brucei* grown in axenic cultures. However, initial growth curves of these cell lines demonstrated a slightly increased doubling time compared to the parental wildtype (WT) BF 427 *T. brucei* cells. This assay was performed in HMI-11 media containing the antibiotics used to select for parasites that had

integrated the ectopic DNA that replaced each allele. Since there is no way for the cells to regain the deleted gene, these antibiotics are no longer necessary to maintain the cell line. Since it takes energy to express the antibiotic resistance genes, which are probably not 100% efficient at degrading the antibiotics in the media, we repeated these growth curves in media without the antibiotics. Indeed, these new growth curves (Figure 7) suggest that any lag in the doubling time for TbAAC DKO and TbSCoAS DKO was probably due to the presence of the antibiotics in the media. If anything, the DKO cell lines now grow slightly faster than the parental cell line.

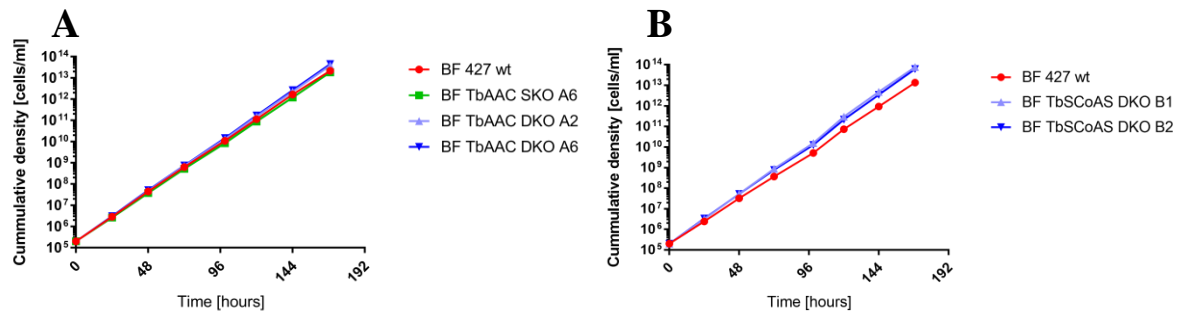


**Figure 7: The calculated cumulative cell density of A) TbAAC DKO or B) TbSCoAS DKO cell lines compared to WT BF 427 *T. brucei*. To maintain the cultures within mid-log growth phase, cell lines were counted daily and split to  $2 \times 10^5$  cells/ml in HMI-11 media without the selectable antibiotics.**

### 3.2 AAC RNAi knockdown in SCoAS double knockout

If TbAAC and TbSCoAS are truly able to compensate for each other in axenic cultures of BF *T. brucei*, then the knockdown of TbAAC in the background of TbSCoAS DKO cells should generate a large growth phenotype. We chose to perform the RNAi of TbAAC because we have an antibody to this mt carrier, making it easier to verify significant protein losses upon RNAi induction. This experiment had previously been performed using an RNAi vector that creates dsRNA by utilizing head-to-head T7 promoter sequences and the ectopic expression of T7 polymerase. However, it was determined that these cells had insufficient knockdown of the target protein. Therefore TbAAC RNAi sequence was cloned into a stem loop RNAi vector that contains two different multiple cloning sites (MSC1 & 2) separated by a fragment of the  $\beta$ -galactosidase gene. This vector, pAZ055, in theory should generate a better knockdown of TbAAC.

#### 3.2.1 Cloning Results

A previous member of the lab had successfully integrated the TbAAC RNAi per fragment into MCS1 of pAZ055. To subclone the RNAi fragment into MCS2, we needed to prepare a midprep of the pAZ055 TbAAC MSC1 vector. This yielded 50ul of plasmid DNA at

4363ng/ul. To verify that this was indeed the correct plasmid, we performed a restriction digest analysis using the enzymes KpnI and BamHI. The digested DNA was then resolved on a 1% TAE agarose gel containing ethidium bromide (Figure 8). The expected sizes of this digest are 5400 nt and 476 nt, thus we verified that we are working with the correct plasmid. The EtBr in the gel allows the DNA to be visualized with a UV light source since it intercalates between the DNA bases. Thus, the upper band is more intense because it has more possible sites for the EtBr to interact. Furthermore, ethidium bromide has a positive charge and thus migrates towards the anode or “up” the gel relative to the migration of the DNA.

This plasmid was then digested with the enzymes XhoI and XbaI, which cut within the MCS2. The digested DNA was resolved on an agarose gel, revealing a single band at the expected size of 5876 nt (Figure 10) and the larger plasmid backbone DNA molecule was extracted. The resulting linearized vector was 68.8 ng/ul.

Next more TbAAC RNAi PCR products needed to be generated to insert into the MCS2. Since it is a short fragment and the accuracy of the polymerase was not of concern, a simple Taq polymerase was used for the 50ul PCR reaction. When the PCR cycles were completed, the end products were resolved on another agarose gel (Figure 9) revealing a fragment of expected size (~500nt). This fragment was then also digested with XhoI and XbaI and then cleaned up using a kit from Sigma. This resulted in 17.2ng/ul of the TbAAC RNAi PCR product.

These digested DNA molecules were then ligated to create pAZ055 TbAAC RNAi vector (1:3 molar ratio of plasmid to insert, 10x buffer, T4 DNA Ligase). Plasmids were isolated from several bacterial transformant colonies and then digested with restriction enzymes to verify that the vector was properly assembled. Unfortunately, the resulting agarose gel did not yield clear results (three bands were expected: ~5400, ~410 and ~480 instead of 2) possibly due to a faulty KpnI enzyme (Figure 11). However, the sequencing data obtained with AZ0461 and AZ0462 primers revealed the pAZ55 vectors with properly inserted TbAAC RNAi in MCS2.

NotI linearized pAZ055 TbACC RNAi plasmid was transfected into the BF TbSCoAS DKO cell line and selected with phleomycin. The transfection produced several viable clonal cell lines, but only one was analyzed for a growth phenotype upon tetracycline induced RNAi (Figure 12). This cell line displayed a significant growth phenotype that would suggest these two pathways do indeed overlap in culture and that one of them is required to supply the mitochondrion with ATP. It was also observed that the rate of proliferation of the uninduced culture also grew slower than the parental cell line, suggested that there might have been a problem with leaky dsRNA expression. Furthermore, this cell line reverted to a normal growth rate soon after the growth curve was completed and this newly adapted cell line was no longer sensitive to tetracycline.

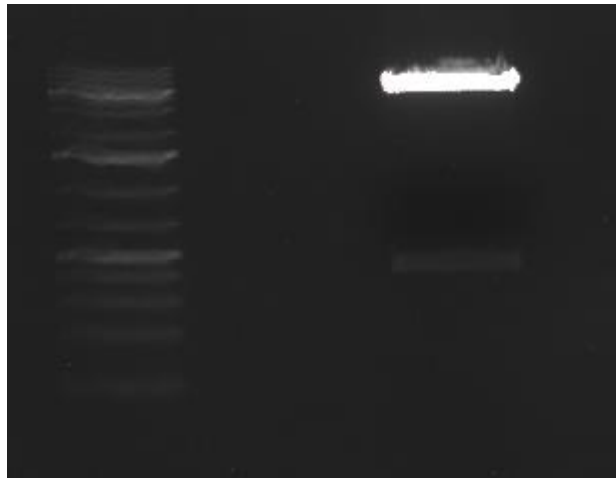


**Figure 8: Plasmid digest with KpnI and BamHI.**

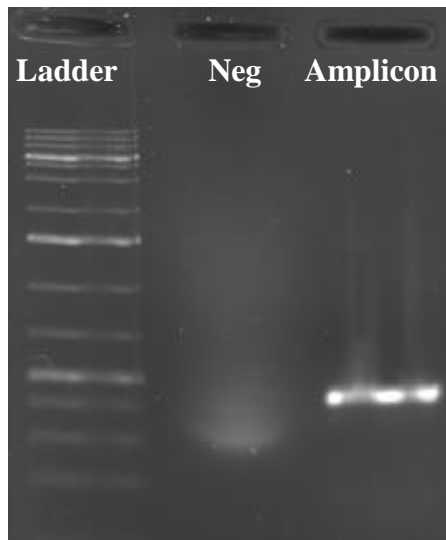


**Figure 9: TbAAC RNAi amplicon resolved on 1% agarose gel. M – 1Kb plus DNA ladder; negative control consists of a PCR reaction without gDNA.**

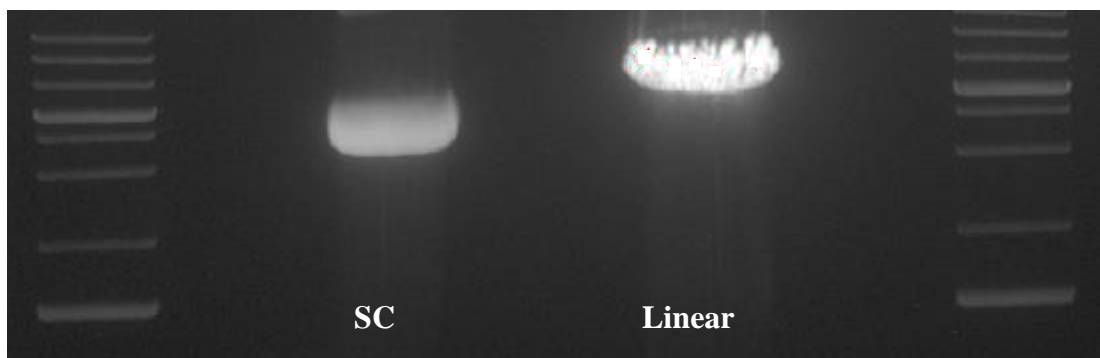


**Figure 10: Agarose gel. The difference between supercoiled plasmid and linearized plasmid.**

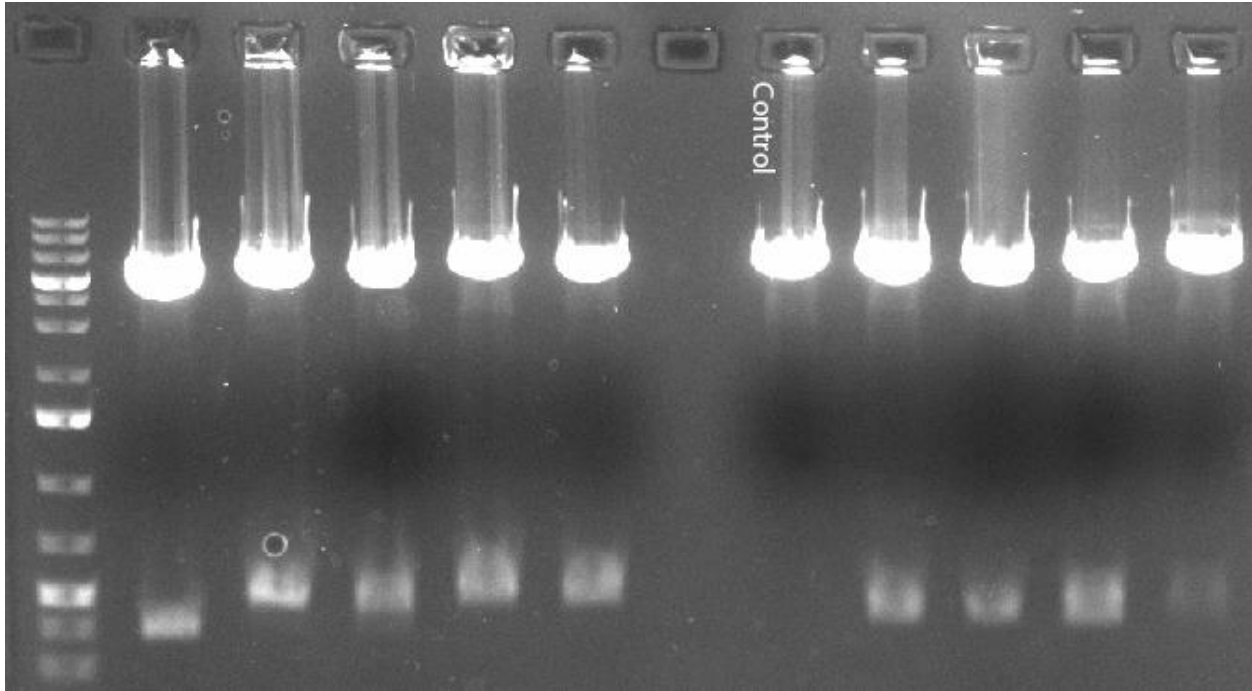


Figure 11: Digestion analysis of the completed plasmid (KpnI and BamHI).

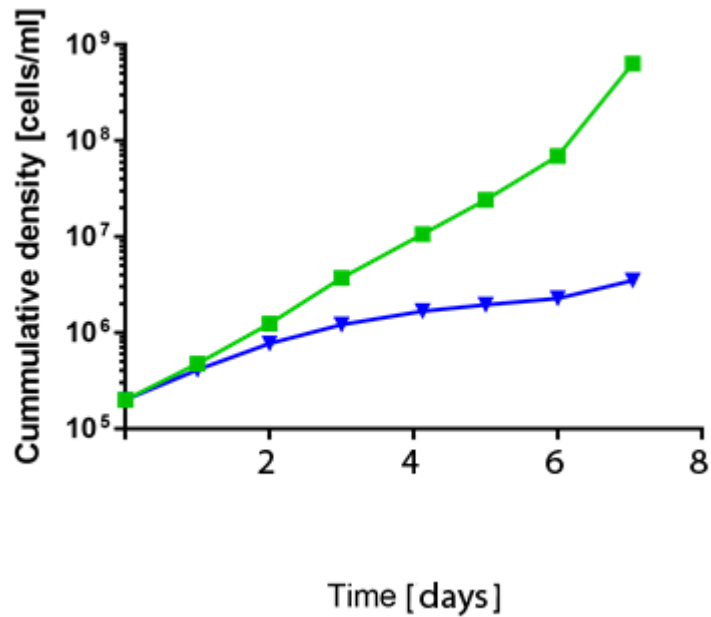
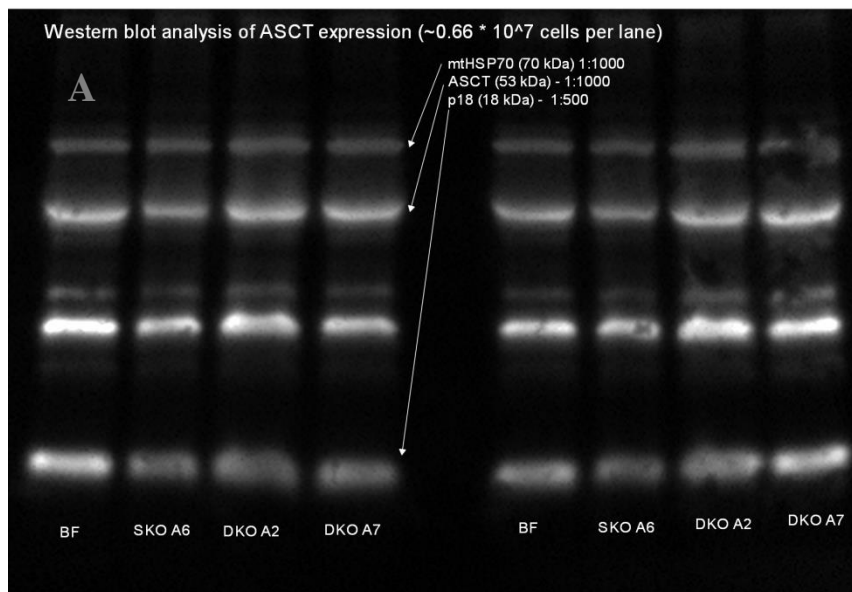


Figure 12: Growth curve of tetracycline induced TbAAC RNAi in TbSCoAS DKO cells. Blue – tetracycline induced RNAi, Green - non-induced culture.

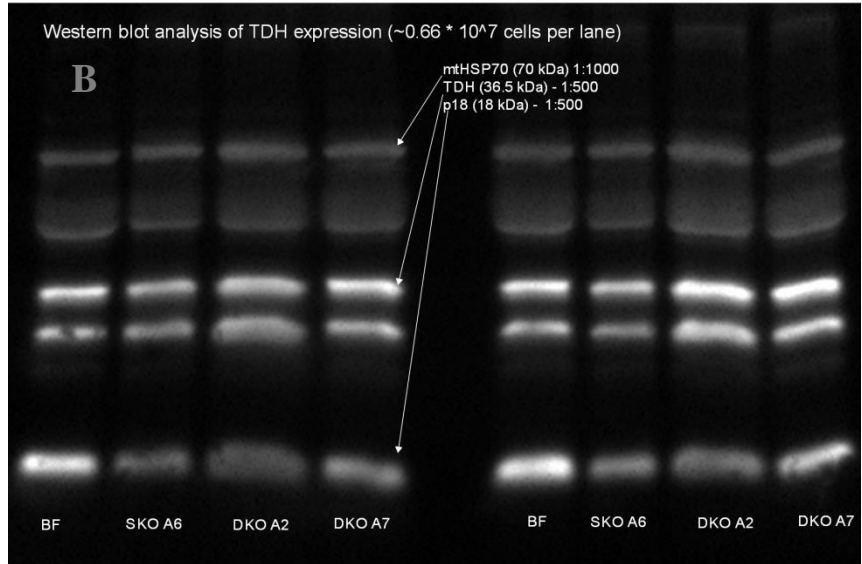
### 3.3 Expression levels of enzymes involved in BF mt bioenergetics.

Since the activity of the  $F_0F_1$ -ATPase is essential in BF *T. brucei*, there must be a source of mt ATP. The previous data would suggest that TbAAC and TbSCoAS can compensate for each other in cells grown in culture. The best evidence for this hypothesis is

work done by others in the lab that show that TbSCoAS DKO cells have an increased sensitivity to CATR, an inhibitor of TbAAC. If ATP cannot be imported from the cytosol in the TbAAC DKO cell line, it is possible that the mt substrate phosphorylation enzymatic pathways are upregulated to compensate for this loss of ATP. Potentially, the expression levels of key proteins in these processes might be increased compared to WT BF *T. brucei*. Therefore, we decided to perform western blot analyses on TbAAC DKO WCLs probed with antibodies against TDH and ASCT (antibodies were a generous gift from the Bringaud lab, University of Bordeaux). The expression levels of neither enzyme seems to change between the WT BF cells and TbAAC DKO cells (Figure 13 A and B). However, it is possible that the mt ATP levels correlate with the abundance of the ATP consumer, F<sub>0</sub>F<sub>1</sub>-ATPase. Since the absence of TbAAC might affect the stability or amount of F<sub>0</sub>F<sub>1</sub>-ATPase, we also probed the blots with an essential F<sub>1</sub>-ATPase subunit, p18. It appears that p18 is reduced in the TbAAC DKO cells, which complicates the interpretation of the unchanged TDH and ASCT expression levels. The unchanged expression levels of mtHSP70 indicate that this decrease in p18 is not due to a global mt protein effect.



**Figure 13:** Western blot analysis of WCLs generated from WT BF 427 cells (WT BF), TbAAC SKO clone A6 or TbAAC DKO clones A2 and A7. The blots were sequentially probed with the antibody dilutions listed in Table 4 with ASCT featured in A) and TDH in B). The WCLs for each sample represent  $0.66 \times 10^7$  cell equivalents.



A similar analysis was performed with the TbSCoAS DKO cell lines (Figure 14). Again, it appears that ASCT levels do not change despite the absence of the upstream TbSCoAS enzyme. In contrast to the TbAAC DKO cells, the levels of p18 remain constant. Furthermore, despite the significant increase in sensitivity to CATR, TbAAC expression appears unchanged. Finally, mtHSP70 again serves as a loading control for the various samples.

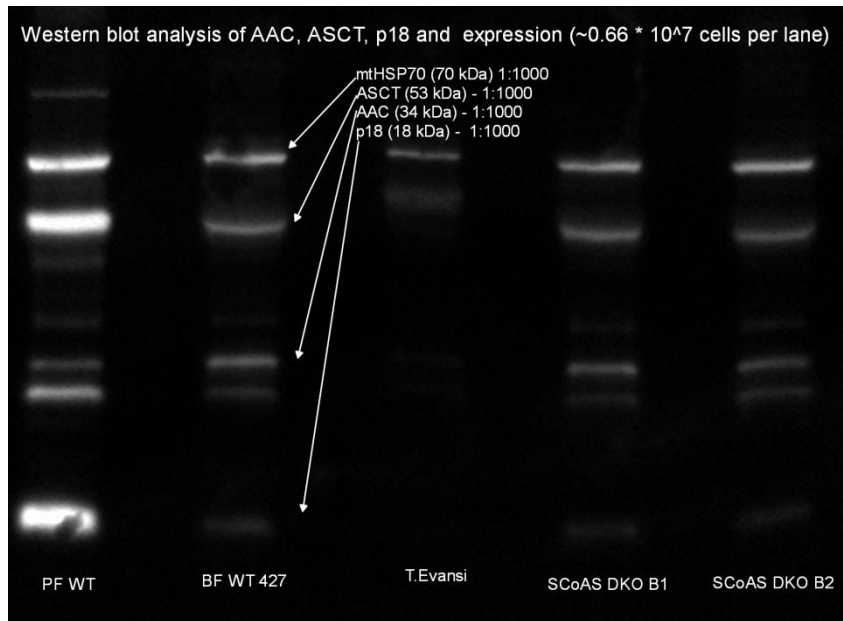


**Figure 14:** Western blot analysis of WCLs generated from WT BF 427 cells (WT BF) and TbSCoAS DKO clones B1 and B2. The blots were sequentially probed with the antibody dilutions listed in Table 4. The WCLs for each sample represent  $0.66 \times 10^7$  cell equivalents.

### 3.4 TbAAC DKO and TbSCoAS DKO $\Delta\psi_m$ measurements.

The presumed function of either TbAAC or TbSCoAS is to supply the BF *T. brucei* mitochondrion with ATP that can be consumed by  $F_0F_1$ -ATPase to generate the essential  $\Delta\psi_m$ . Therefore, we assayed the ability of each DKO cell line to maintain the  $\Delta\psi_m$  compared to WT levels. This was performed in live cells using the fluorescent dye TMRE. We observed that the TbAAC DKO cell lines have about a 20% decrease in their  $\Delta\psi_m$  (Figure 15A). This would suggest that TbAAC is contributing to the  $\Delta\psi_m$  in some capacity in the WT cells, but there is probably another source of mt ATP that can compensate for the loss of TbAAC. In contrast, the  $\Delta\psi_m$  of the TbSCoAS DKO cell line actually increases slightly compared to the levels measured in WT BF cells (Figure 15B). This demonstrates that axenic BF *T. brucei* can maintain their  $\Delta\psi_m$  without the ability to perform mt substrate phosphorylation. Treating the cells with FCCP, a proton ionophore, destabilized the  $\Delta\psi_m$ . This demonstrates that the fluorescence measured was due to the mt electrochemical gradient.

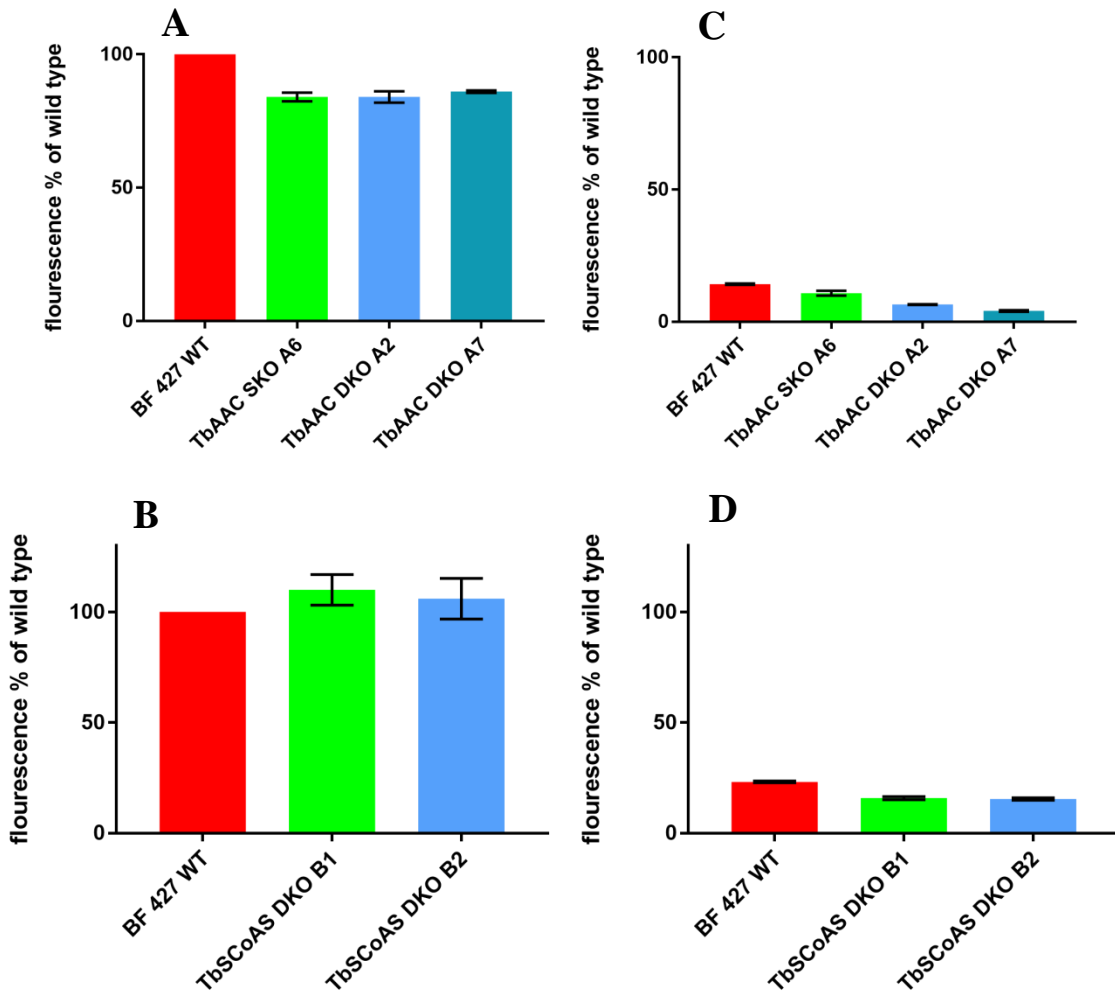
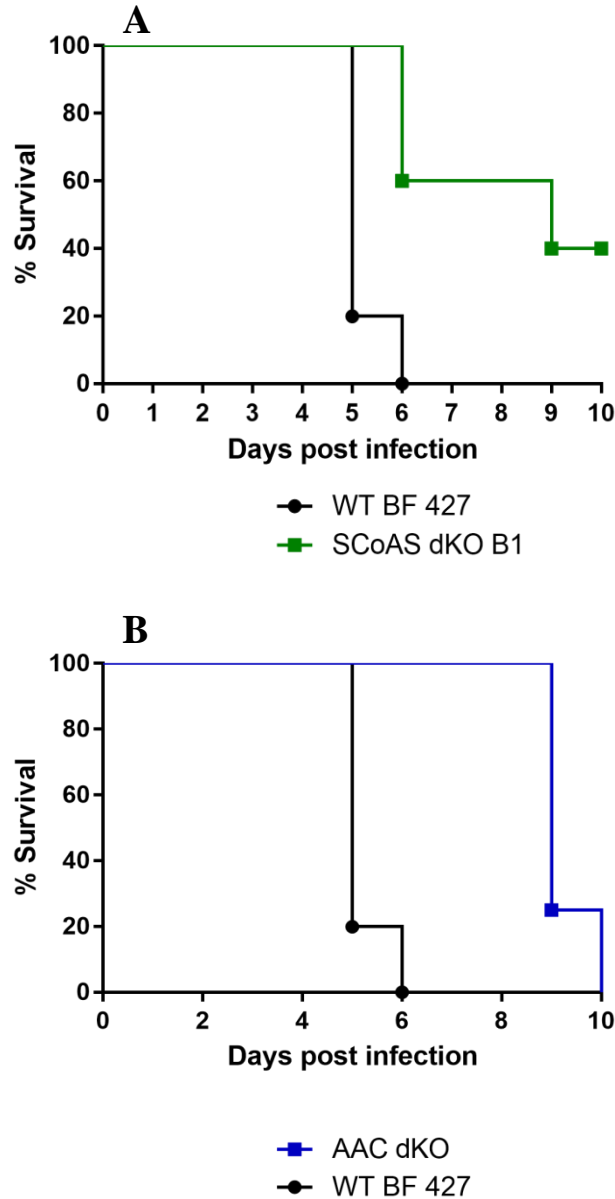


Figure 15: The  $\Delta\psi_m$  of A) TbAAC or B) TbSCoAS DKO cell lines stained for 30 minutes with 60nM TMRE and analyzed on the FACS Canto II flow cytometer. Cells from the same flask C) TbAAC or D) TbSCoAS were also treated with TMRE and 20uM FCCP to verify that the measured values were due to the mt electrochemical potential. Relative values are expressed as a % of the WT levels and are the average of measurements taken from three independent experiments.

### 3.5 Loss of TbSCoAS but not TbAAC decreases the virulence of *T. brucei* in mice

While the TbAAC DKO and TbSCoAS DKO cell lines demonstrated no growth phenotype when grown in media rich with various carbon sources, the energetic demands of the parasite likely increase when replicating in a mammalian host with an active immune system. Therefore,  $1 \times 10^5$  parasites of the various cell lines were injected into mice and their parasitemia was monitored daily (Figure 16). The resulting data was then used to generate survival analysis curves. Mice infected with parasites lacking TbAAC, still succumbed to infection, albeit on the

second wave of parasitemia. Therefore, while the TbAAC DKO *T. brucei* might have a slightly decreased fitness, they are still capable of overwhelming their mammalian host. While not completely conclusive, this seems in contrast to the TbSCoAS DKO parasites, where two of the five mice completely cleared the *T. brucei* infection. This preliminary data needs to be repeated, but it suggests that in the mammalian host, TbSCoAS is more important for the survival of the parasite than TbAAC.



**Figure 16: Survival analysis curves of BALB/c mice infected with  $1 \times 10^5$  A) TbAAC DKO or B) TbSCoAS DKO parasites. The same number of BF WT 427 *T. brucei* parasites were injected into a control group of mice. C) The daily parasitemia counts for several representative mice infected with TbAAC DKO *T. brucei*.**

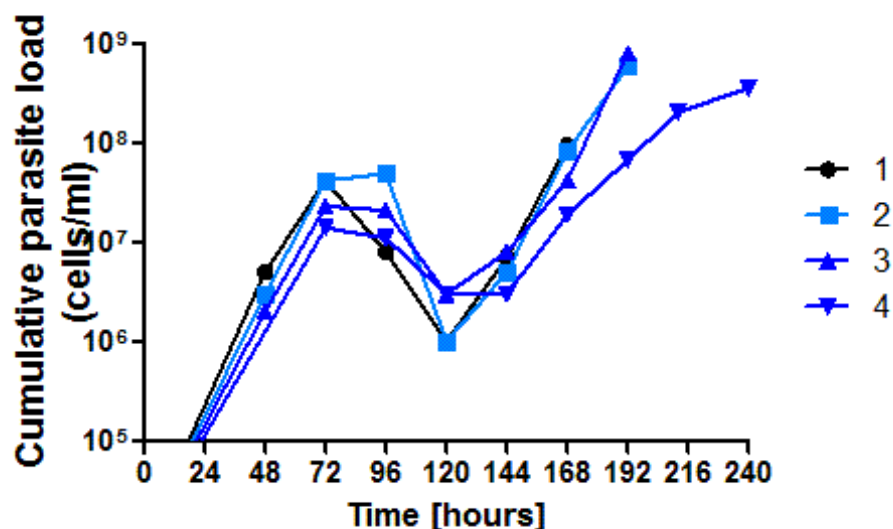


Figure 17: Parasitemia of mice infected with AAC DKO cell line.

### 3.6 Metabolomic analysis.

Metabolomics is a powerful way to glean information about which biochemical pathways are active in a living cell. An attempt of such analysis was carried out on our cell lines to determine if the absence of TbAAC stimulates pathways that would generate ATP via mt substrate phosphorylation. Several different experiments were performed with different cell lines and carbon sources (Table 7).

Table 7: Types of metabolomics experiments performed.

Experiment type	Clones involved	Carbon sources used
1	BF WT427, AAC DKO, SCoAS DKO	Glucose, Glucose-u13
2	BF WT427, AAC KD in SCoAS DKO IND 5 days post tet/NON IND	Glucose, Glucose-u13+Threonine
3	BF WT427, AAC KD in SCoAS DKO IND 7 days post tet/NON IND	Glucose, Glucose-u13, Glucose-u13+Threonine
4	BF WT427, AAC DKO, SCoAS DKO	Glucose-u13, Glucose-u13+Glutamate, Glucose-u13+Glutamine

### 3.6.1 Measurements

Cells were closely monitored during their incubation period with the various carbon sources to optimize the time to harvest the excreted metabolites found in the media. The NMR spectra of these samples were measured. Due to complexity of the quantification procedure, only the results that looked promising were further quantified. Among the samples that did not yield interpretable results were the samples with glutamate and glutamine. Superficial examination of the spectra showed no change in the production of acetate and succinate. Several threonine samples did not contain threonine, possibly due to an error during the sample preparation. Furthermore, the samples incubated with the amino acids were not considered since they did not provide any new insights compared to the glucose samples.

The results were compiled from the data extracted from the spectra produced by the cells incubated with unlabeled glucose (Figure 18). That experiment enabled a comparison of the acetate excretion levels in the BF WT 427, TbAAC DKO, TbSCoAS DKO, TbAAC RNAi/TbSCoAS DKO cell lines. However, after the experiment was performed, we realized that the BF WT 427 was actually the TbSCoAS DKO cell line. That matter is further investigated in the discussion.

The most significant finding from these measurements concerns the acetate production, since we would expect this to increase in the TbAAC DKO cell line due to an increased demand for ATP from the TbSCoAS pathway (Figure 1). With more or less consistent pyruvate levels, showing that the cytosolic metabolism of the cells does not vary significantly over the various cell lines, the acetate excretion of the TbAAC DKO line is about 8 times higher than that of the wild type (Table 8).

Table 8: Summary of excreted metabolites by cell lines incubated in unlabeled glucose. Quantities are measured in nmoles/hour/10<sup>8</sup> cells.

Cell Line	BF 427 WT		BF KO AAC		BF KO SCoAS		KOSCoAS/RNAiAAC NI		KOSCoAS/RNAiAAC I	
	15		8		8		6		6	
Number of samples	Mean	SD	Mean	SD	Mean	SD	Mean	SD	Mean	SD
Succinate	140	23	187	80	158	49	113	36	131	11
Pyruvate	7462	716	6588	1891	7461	1041	7263	1373	6806	428
acetate	34	10	264	128	36	5	32	8	35	8
Alanine	878	84	784	227	885	225	855	157	806	53
Lactate	521	357	379	331	479	198	358	95	552	339
<b>Total</b>	<b>9036</b>	<b>797</b>	<b>8202</b>	<b>2044</b>	<b>9018</b>	<b>1063</b>	<b>8621</b>	<b>1618</b>	<b>8330</b>	<b>217</b>

<b>Ratio Pyruvate/Acetate</b>	218	25	210	226	197
-------------------------------	-----	----	-----	-----	-----

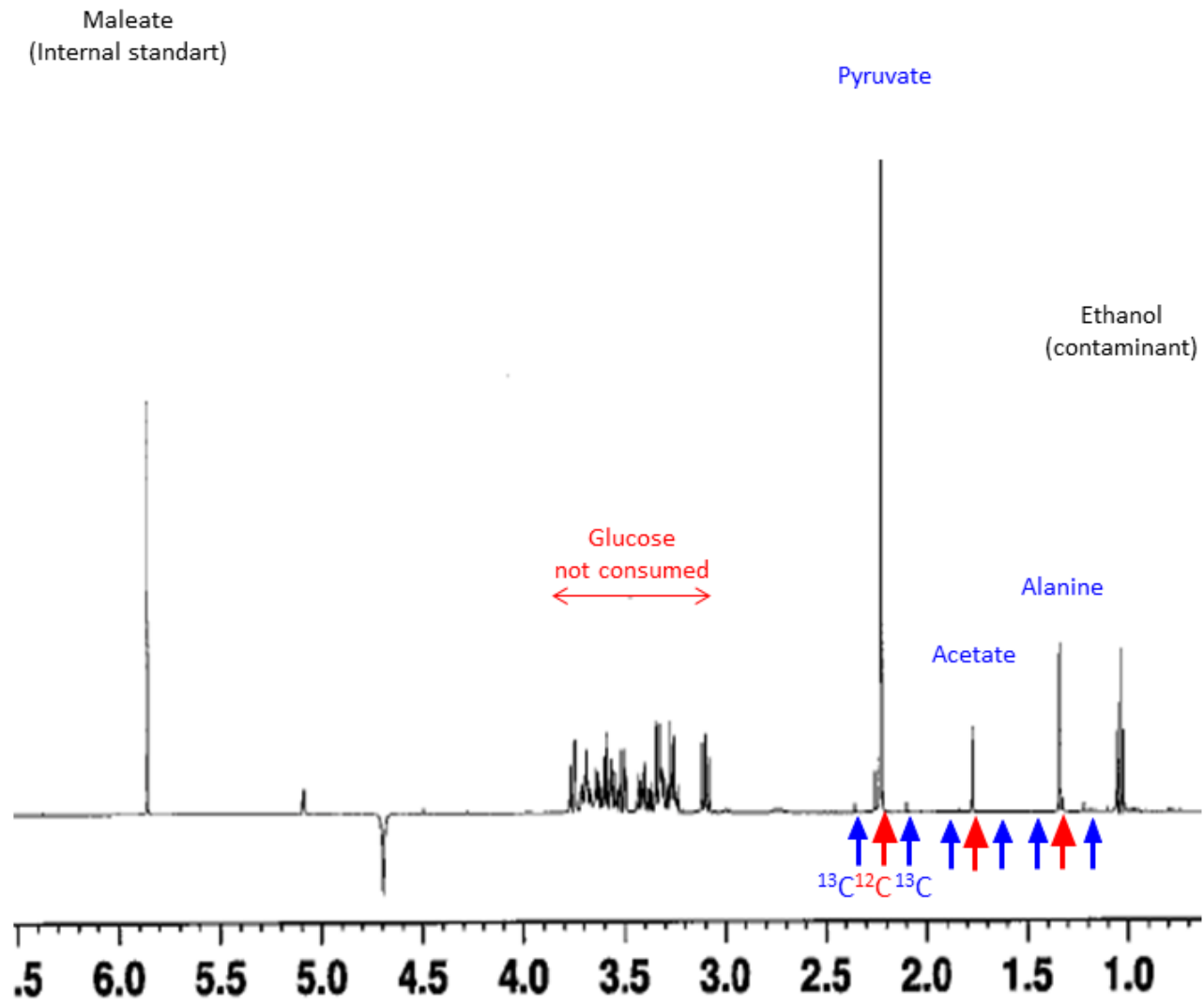


Figure 18: Annotated example of NMR spectrum of a sample incubated with unlabeled glucose.

## 4 Discussion

While most of the data still needs to be repeated and verified, there is a strong suggestion that in culture, BF WT *T. brucei* can supply the mitochondrion with ATP either via TbSCoAS and mt substrate phosphorylation or through the import of cytosolic ATP by TbAAC. The ability to generate independent DKO cell lines for both TbAAC and TbSCoAS suggests an overlapping function of these proteins in axenic cultures. This is further supported by the mild changes observed in the  $\Delta\psi_m$  for both cell lines. In addition, our limited metabolomics data suggests that acetate production and thus ATP production via mt substrate phosphorylation is drastically elevated in the TbAAC DKO cell line. We came tantalizingly close to directly demonstrating this complementation when we temporarily observed a significant growth phenotype when TbAAC was depleted in the TbSCoAS DKO cell line. Perhaps the most revealing data to indicate that the BF mitochondrion can produce its own ATP involves the mouse studies that demonstrate that some animals are able to clear the TbSCoAS DKO parasites, but not the TbAAC DKO infection.

When the TbAAC and TbSCoAS DKO cell lines were originally generated, they demonstrated a slight increase in their doubling time. These original measurements were done in media containing the antibiotics required to select for positively transfected parasites, but these are no longer required once both alleles have been removed. The new growth curves have shown that the TbAAC and TbSCoAS knockout lines have growth which is practically equivalent to that of the wild-type cell lines in the antibiotic free media. Therefore, the previously observed growth defects were most likely due to the antibiotics, not the lack of the gene product. The viability and rapid growth rate of these DKO cell lines demonstrates that the mitochondrion bioenergetics of this parasite can rapidly switch between biochemical pathways when they are growing in nutrient rich media, indicating that the mt SUBPHOS pathways and TbAAC can compensate for each other's absence.

If the activities of TbAAC and TbSCoAS are coordinated, it might be possible to detect increases in the expression levels of enzymes preceding TbSCoAS in the TbAAC DKO cell line. However, the only antibodies available to us, those specific to TDH and ASCT, did not detect a change in protein levels. We have since learned through personal communication with the Bringaud lab at the University of Bordeaux, that the biochemical pathway involving TDH is probably channeled to ACH to produce acetate, thus increased activity of TDH would not produce significant amount of ATP via TbSCoAS. The lack of change in the expression of ASCT suggests that if more mt ATP is being produced in the mitochondrion when TbAAC is absent, then this could be due to increased glutamate catabolism that leads to the generation of succinate and ATP by TbSCoAS. However, we are not able to measure the in vivo rate of these enzymes and it might be that they are capable of generating greater amounts of ATP without increasing the abundance of the protein. This could be achieved by increased substrate

availability, greater  $V_{\max}$  or  $K_m$  values of the enzyme or some channeling mechanism. Therefore, we are unfortunately not able to make any significant conclusions from this data.

The possible interplay between TbAAC and TbSCoAS is also suggested in the  $\Delta\psi_m$  measurements made in the TbAAC and TbSCoAS DKO cell lines. Since the action of TbAAC is reversed in the BF mitochondrion, TbAAC contributes to the membrane potential by exchanging  $ATP^{4-}$  from the cytosol for  $ADP^{3-}$  from the mt matrix, thus creating an equivalent of one positive charge transfer to the mt membrane inner space. When TbAAC is absent, it is possible that TbSCoAS is able to match the total WT levels of mt ATP, but this electrogenic exchange by TbAAC will be absent and could account for ~15% of the  $\Delta\psi_m$ . At the same time, the  $\Delta\psi_m$  of the SCoAS DKO cells appears to be slightly higher than that of the parental cell line. If this increase is truly significant, it could be related to either an increase in TbAAC expression, acetate export decrease or increased activity of  $F_0F_1$ -ATPase. Unfortunately, it would be very difficult to measure the rate of ATPase activity under the conditions of a live cell, but there is no observed increase in the amount of acetate excretion compared to the data published for the parental cell line (Mazet, et al. 2013). While there is no clear indication for increased TbAAC expression in the western blot analyses (Figure 14), we do know that this cell line has a significantly increased sensitivity to CATR. This suggests that the cell is now relying more heavily on this carrier to import ATP into the mitochondrion when TbSCoAS is absent. Without any increase in TbAAC expression levels, perhaps the rate of TbAAC is increased and there is a greater electrogenic contribution to the  $\Delta\psi_m$ .

The incomplete metabolomics data also offers hints that TbSCoAS is active in the BF *T. brucei* mitochondrion. Unfortunately, the control group for the metabolomics studies turned out, by all indications, to be TbSCoAS DKO instead of the parental WT 427 strain. This could have happened due to cross-contamination during the sample preparation or at any point prior. This set of experiments will have to be repeated with a proper positive control. In addition, the experiments with glutamine and glutamate did not work properly as it appears that these amino acids were not adequately taken up by the cells for some reason. Finally, the threonine experiments also failed to produce meaningful results. Sadly, these two circumstances preclude us from reaching any significant conclusions about the relationship between the two SUBPHOS pathways within the mitochondrion of the parasite. However, a small amount of useful data has been produced. For instance, it has been determined that the pyruvate/acetate excretion ratio in the TbAAC DKO cells is sharply decreased as a consequence of an almost tenfold increase in acetate production as compared to the TbSCoAS DKO cells. This evidence supports the hypothesis of the complementary role of substrate phosphorylation as a valid energy source for the BF mitochondrion. The excretion of other metabolites is largely unaffected and is similar in the two knockouts. Metabolomic analysis of the TbAAC KD in TbSCoAS DKO cell line did not produce significant differences between the induced and non-induced cells. However, this cell line had already become largely insensitive to the tetracycline RNAi induction and displayed a much reduced growth phenotype at the time of the metabolomics assays.

The generation of an efficient TbAAC knockdown in the TbSCoAS DKO cell line would significantly help us to understand if TbAAC and TbSCoAS can compensate for each other in nutrient rich media. Previous attempts to knockdown TbAAC using the head-to-head p2T7 RNAi plasmid failed to generate a robust knockdown of the target gene product. Thus, these cells failed to produce any growth phenotype when the RNAi was induced. Therefore, we decided to use the stem loop RNAi vector pAZ055, which should theoretically produce a more significant depletion of TbAAC. While we were able to select a few clonal cell lines, only one was assayed for a growth phenotype upon RNAi induction. This cell line finally demonstrated the drastic growth phenotype that would be expected if TbAAC and TbSCoAS overlapped in function and were the only sources of mt ATP. However, this cell line already had a retarded growth rate even when the RNAi was turned off. This might signify that there was leaky RNAi expression that was inhibiting the growth rate of the cells or it might have meant that the cells were still under the selection process. Either way, the cell line soon reverted back to near normal proliferation rates and no longer demonstrated a growth phenotype when induced with tetracycline. While the pAZ055 stem loop RNAi vector should produce more robust dsRNA, it is integrated into the ribosomal RNA spacer locus, an area of high transcription activity. This might explain why we get more clones when we transfect with the p2T7 RNAi vector, which integrates into the silent minichromosome locus. If the parasite depends on either the TbAAC or TbSCoAS to provide the BF mitochondrion with ATP, it might be technically demanding to create the TbAAC RNAi TbSCoAS DKO cell line. One alternative might be to create a regulatable TbAAC conditional KO in the TbSCoAS DKO cell line. While we would have to swap some additional antibiotic resistance markers, this should present a better opportunity to more tightly regulate the expression of these proteins and determine if the two protein functions are complementary and necessary to the BF *T. brucei*.

The mouse studies also provide preliminary results that lend credence to the BF *T. brucei* mitochondrion being an ATP producing organelle. Since all the mice infected with the TbAAC DKO parasites succumbed to the disease, it suggests that these cells must be able to generate mt ATP in order to maintain the essential  $\Delta\psi_m$ . However, these mice were able to suppress the first wave of parasitemia, so it is possible that the TbAAC DKO parasites might have a decreased fitness. It is also possible that these mice were injected with fewer parasites, as it is typical to see multiple waves of parasitemia when the mice are infected with low numbers of *T. brucei*. The data for the mice infected with the TbSCoAS DKO cells indicates even more evidence that the parasites have a decreased virulence as two of the mice were able to completely clear the *T. brucei* infection and one of the other mice needed to be euthanized only after the second wave of parasitemia. Unfortunately, the daily parasitemia counts for these animals is incomplete and these studies will also have to be repeated to verify the outcome. However, it is possible that the higher energetic demands of a parasite evading the active immune system of its host means that there is a smaller pool of ATP produced by glycolysis available in the cytosol for TbAAC to import into the mitochondrion when TbSCOAS is absent. Overall the data collected during the course of this project, whenever reliable, aligns

well with the model proposed in (Zíkova, Verner and Nenarokova 2017), in which the SUBPHOS pathways of the mitochondria work alongside TbAAC to supply ATP to the BF *T. brucei* mitochondrion.

## 5 References

*Reagent recipes of Laboratory of Molecular Biology of Protists (unpublished)*. 2015.

Barret, MP, IM Vincent, RJ Burchmore, AJ Kazibwe, and E Matovu. "Drug resistance in human African trypanosomiasis." *Future Microbiol* 6, 2011: 1037-1047.

Bio-Rad Laboratories. "ChemiDoc MP System with Image Lab Software Instruction Manual." 2012.

Bochud-Alleman, N, and A Schneider. "Mitochondrial substrate level phosphorylation is essential for growth of procyclic *Trypanosoma brucei*." *J Biol Chem* 277, 2002: 32849-32854.

Bringaud, F, C Ebikeme, and M Boshart. " Acetate and succinate production in amoebae, helminths, diplomonads, trichomonads and trypanosomatids: common and diverse metabolic strategies used by parasitic lower eukaryotes." *Parasitology* 137, 2010: 1315-1331.

Bringaud, F, L Riviere, and V Coustou. "Energy metabolism of trypanosomatids: adaptation to available carbon sources." *Mol Biochem Parasitol* 149, 2006: 1-9.

Bringaud, Frederic, Marc Biran, Yoann Millerioux, Marion Wargnies, Stefan Allman, and Muriel Mazet. "Combining reverse genetics and nuclear magnetic resonance-based metabolomics unravels trypanosome-specific metabolic pathways." *Molecular Microbiology*, March 05, 2015: 917-926.

Cannata, Joaquin J. B., and Juan Jose Cazzulo. "The Aerobic Fermentation of Glucose by *Trypanosoma cruzi*." *Comp. Biochem. Physiol.*, February 21, 1984: 297-308.

Castellani, Sir Aldo, Sir David Bruce, and David Nunes Nabarro. *Reports of the Sleeping Sickness Commission*. Harrison and Sons, 1903.

Colasante, Claudia, P. Pena Diaz, Christine Clayton, and Frank Voncken. "Mitochondrial carrier family inventory of *Trypanosoma brucei brucei*: Identification, expression and subcellular localisation." *Molecular & Biochemical Parasitology*, 2009: 104-117.

Coulter, Wallace H. Means for counting particles suspended in a fluid . US Patent US2656508A. 08 27, 1949.

- Coustou, V, Biran M, M Breton, F Guegan, L Riviere, and et al. "Glucose-induced remodeling of intermediary and energy metabolism in procyclic *Trypanosoma brucei*." *J Biol Chem* 283, 2008: 16342-16354.
- Creek, Darren J., Brunda Nijagal, Dong-Hyun Kim, Federico Rojas, Methews Keith R., and Barret Michael P. "Metabolomics Guides Rational Development of a Simplified Cell Culture Medium for Drug Screening against *Trypanosoma brucei*." *Antimicrobial Agents and Chemotherapy*, 2013: 2768-2779.
- Cross, George. *Trypanosome pedigrees*. April 22, 2010.  
[http://tryps.rockefeller.edu/trypsru2\\_pedigrees.html](http://tryps.rockefeller.edu/trypsru2_pedigrees.html) (accessed April 29, 2017).
- Dubey, R C. "Advanced Biotechnology." 199. S. Chand Publishing., 2014.
- Embley, T. Martin, and William Martin. "Eukaryotic evolution, changes and challenges." *Nature* (Nature Publishing Group) 440 (03 2006): 623-630.
- Gabaldon, T, ML Ginger, and PA Michels. "Peroxisomes in parasitic protists." *Mol Biochem Parasitol* 209, 2016: 35-45.
- Gnipová, Anna, Karolína Šubrtová, Brian Panicucci, Anton Horváth, Julius Lukeš, and Alena Zíková. "The ADP/ATP Carrier and Its Relationship to Oxidative." *Eukaryotic Cell*, March 2015.
- Hirumi H, Hirumi K. "Continuous cultivation of *Trypanosoma*." *J.Parasitol.*, 1989: 985-989.
- Horn, David. "Antigenic variation in African trypanosomes." *Mol Biochem Parasitol*, 2014: 123-129.
- Kedrov, A, AM Hellawell, A Klosin, RN Broadhurst, ER Kunji, and et al. "Probing the interactions of carboxy-atractyloside and atractyloside with the yeast mitochondrial ADP/ATP carrier." *Structure* 18, 2010: 39-46.
- MacGregor, P, B Szoor, NJ Savill, and KR Matthews. "Trypanosomal immune evasion, chronicity and transmission: an elegant balancing act." *Nat Rev Microbiol* 10, 2012: 431-438.
- Matthews, KR. "25 years of African trypanosome research: From description to molecular dissection and new drug discovery." *Mol Biochem Parasitol* 200, 2015: 30-40.
- Mazet, Muriel, et al. "Revisiting the Central Metabolism of the Bloodstream Forms of *Trypanosoma brucei*: Production of Acetate in the Mitochondrion Is Essential for Parasite Viability." *PLoS Negl Trop Dis*, 2013.

- Nagle, AS, S Khare, AB Kumar, F Supek, and A Buchynskyy. "Recent developments in drug discovery for leishmaniasis and human African trypanosomiasis." *Chem Rev* 114, 2014: 11305-11347.
- National Center for Biotechnology Information. *Carbonyl cyanide p-trifluoromethoxyphenylhydrazone* . 03 25, 2005.  
<https://pubchem.ncbi.nlm.nih.gov/compound/3330> (accessed 03 29, 2018).
- Pena Diaz, Priscila, et al. "Functional Characterization of TbMCP5, a Conserved and Essential ADP/ATP Carrier Present in the Mitochondrion of the Human Pathogen *Trypanosoma brucei*." *J. Biol. Chem.*, 2012: 41861-41874.
- Read, LK, J Lukes, and H Hashimi. "Trypanosome RNA editing: the complexity of getting U in and taking U out." *Wiley Interdiscip Rev RNA* 7, 2016: 33-51.
- Ruprecht, JJ, AM Hellawell, M Harding, PG Crichton, AJ McCoy, and et al. "Probing the interactions of carboxy-atractyloside and atractyloside with the yeast mitochondrial ADP/ATP carrier." *Structure* 18, 2010: 39-46.
- Schnauffer, A, GD Clark-Walker, AG Steinberg, and K Stuart. "The F1-ATP synthase complex in bloodstream stage trypanosomes has an unusual and essential function." *EMBO J* 24, 2005: 4029-4040.
- Sigma Aldrich Co. "GenElute(tm) HP Plasmid Midiprep Kit User Guide." 2009.
- . "Product Information GenElute Gel Extraction Kit." n.d.
- . "Product Information GenElute PCR Clean-Up Kit." n.d.
- Simarro, PP, A Diarra, JA Ruiz Postigo, JR Franco, and JG Jannin. "The human African trypanosomiasis control and surveillance programme of the World Health Organization 2000-2009: the way forward." *PLoS Negl Trop Dis* 5: e1007, 2011.
- Smith, Terry K., Frederic Bringaud, Derek P. Nolan, and Luisa M. Figueiredo. "Metabolic reprogramming during the *Trypanosoma brucei* lifecycle." *F1000 research*, 2017.
- Springett, R, MS King, PG Crichton, and ERS Kunji. "Modelling the free energy profile of the mitochondrial ADP/ATP carrier." *Biochim Biophys Acta* 1858, 2017: 906-914.
- Taleva, Gergana. *Literature review: Bioenergetics of the Trypanosoma brucei bloodstream form*. Literature review, Ceske Budejovice: University of South Bohemia, 2016.
- Thermo Fischer Scientific. "PRODUCT INFORMATION THERMOFISCHER SCIENTIFIC Gene Ruler 1kB Plus DNA Ladder." 2012.

- Traba, J, J Satrustegui, and A del Arco. "Transport of adenine nucleotides in the mitochondria of *Saccharomyces cerevisiae*: interactions between the ADP/ATP carriers and the ATP-Mg/Pi carrier." *Mitochondrion* 9, 2009: 79-85.
- Van Weelden, SW, JJ Van Hellemond, FR Opperdoes, and AG Tielens. "New functions for parts of the Krebs cycle in procyclic *Trypanosoma brucei*, a cycle not operating as a cycle." *J Biol Chem* 280, 2005: 12451-12460.
- Vickerman, K. "Developmental cycles and biology of pathogenic trypanosomes." *Br Med Bull* 41, 1985: 105-114.
- . "Polymorphism and mitochondrial activity in sleeping sickness trypanosomes." *Nature* 208, 1965: 762-766.
- World Health Organization. *The parasite*. August 05, 2016.  
[http://www.who.int/trypanosomiasis\\_african/disease/parasite/en/](http://www.who.int/trypanosomiasis_african/disease/parasite/en/) (accessed April 23, 2018).
- Zhang, X, J Cui, D Nilsson, K Gunasekera, A Chanfon, and et al. "The *Trypanosoma brucei* MitoCarta and its regulation and splicing pattern during development." *Nucleic Acids Res* 38, 2010: 7378-7387.
- Zikova, A, A Schnauffer, RA Dalley, AK Panigrahi, and KD Stuart. "The F(0)F(1)-ATP synthase complex contains novel subunits and is essential for procyclic *Trypanosoma brucei*." *PLoS Pathog* 5, 2009: e1000436.
- Zikova, A, Z Verner, and A Nenarokova. "A paradigm shift: The mitoproteomes of procyclic and bloodstream *Trypanosoma brucei* are comparably complex." *PLoS Pathog* 13(12): e1006679., 2017.